A Table Top Static Gas Sensing Unit 14

महत्वाकांक्षी भारत को बिजली उपलब्ध करना 26

Bi-monthly • May - June • 2017

ISSN: 0976-2108

# BARC NEWSLETTER

Pipeline inspection gauge

Location of Radiotracer Sampling

# CONTENTS

# Development and Application of Radiotracer Dilution Technique for Flow Rate Measurements

**H.J. Pant, Jayashree Biswal, Sunil Goswami, J.S. Samantray, V.K. Sharma and K.S.S. Sarma**
Isotope and Radiation Application Division
**Shyam Shukla**
Kirloskar Brothers Limited, Yamuna, Survey No. 98 (3-7), Baner, Pune - 411 045

Radiotracer dilution technique for flow rate measurements in pipelines, canals, mountainous rivers, and streams was developed and applied for measurement of water flow rates in a branch canal of M/s Sardar Sarovar Narmada Nigam Limited (SSNNL), Surendranagar, Gujarat and in large diameter pipelines in a power plant at Vishakhapatnam, owned by M/s Hinduja National Power Corporation Limited (HNPCL), Vishakhapatnam, Andhra Pradesh. In case of the M/s SSNNL, Gujarat, the measurements were carried out to quantify the flow rates and validate the efficacy of the Concrete Volute (CV) Pumps used for pumping the water along the canal. Whereas in case of the M/s HNPCL, Andhra Pradesh, the flow rate measurements were carried out to check the calibration of the installed flow meters as well as to validate the efficacy of the Vertical Turbine (VT) pumps used for pumping water through the pipelines. Iodine-131 as potassium iodide was used as radiotracer in both the cases. The flow rates of water were ranging from 20.30±0.29 - 20.62±0.26 $m^3/s$ measured at four different pumping stations along the canal when single CV pump was operated. The measured flow rates were found to be in agreement with the theoretically estimated pumping capacity of a CV pump, i.e. 20 $m^3/s$. The values of the flow rates measured in large diameter pipelines at M/s HNPCL, Visakhapatnam, ranged from 14.10±0.43 - 15.43±0.46 $m^3/s$ with single VT pump in operation and ranged from 24.55±0.78 - 27.51±0.82 $m^3/s$ when two identical VT pumps were operated simultaneously. The measured values of the flow rates were used to validate the efficacy of the pumps, calibrate the flow meters and optimize the pumping operations leading to significant revenue savings to the industries.

## Introduction

The accurate knowledge of flow rates of process material (liquid, gas and solid) in industrial and environmental systems is an essential requirement. The flow rates are usually needed for one or more of the following reasons i.e. calibration of installed flow meters, in situations where flow meters are not installed, material balance, measurement of efficacy of pumps or turbines, distribution of flow in a network of pipes, etc. Generally, the industrial systems where the flow rates are needed to be measured are classified into two categories, namely open channels and closed conduits. Open channels are systems where the stream has a free surface open to the atmosphere such as canals, rivers, streams, sewer lines, effluent channels etc. Flow in closed conduits, such as pipelines is caused by a pressure difference. Various conventional methods such as gravimetric method, hydraulic structure method, velocity-area method or current meter method and slope-hydraulic radius method are used for flow rate measurements in canals, rivers and tunnels [1-8]. None of the above methods can be applied for flow rate measurement in all the situations. The selection of a suitable method for a particular application depends on the type and nature of the system, physical properties of the flowing water, flow patterns of the water, limitations imposed by the design and operating condition of the plant, cost and installation of the equipment. Similarly, various types of flow meters, such as ultrasonic, electromagnetic, acoustic, venturi, pitot tube, etc., are used for flow rate measurements in pipelines [9] in industry. Most of these flow meters have limitations in large diameter pipelines.

Tracer dilution method is one of the most widely used and well-suited for flow rate measurements in canals and large diameter pipelines. The tracer dilution technique can be applied for flow measurements in irregular shaped, large diameter and fully or partially filled pipelines [1-18]. The dilution technique can also be used for flow rate measurement even when the flow path is branched. The tracer used could be either a chemical or a radioactive isotope. Chemical tracers such as fluorescent dye, normal salts are commonly used for measurement of flow rates in canals and pipelines. The measurement of high flow rates using chemical tracer requires large amount of tracers to be injected as they cannot be detected below a few milligram per litre. Injecting a large amount of tracer will affect the flow as well as contaminate the system. The fluorescent dyes such as Rodamine B, though detectable under high dilutions, are generally lost from the water medium through adsorption on the bed, walls and soil in suspension [13]. Some of these drawbacks of chemical tracers could be overcome by using radiotracers. The radiotracers are particularly useful for higher discharge rate (upto 1200 $m^3/s$) measurements with better accuracy owing to their higher detection sensitivity ($10^{-9}$ mg/cc) [11, 12, 14-16]. Because of this property of radiotracers, a few micrograms of radiotracer is sufficient. There is essentially no interference with the system being studied. The present article describes an application of radiotracer dilution technique flow measurements in a canal and large diameter pipelines to evaluate and validate the pumping efficacy of the pumps used for pumping the water and calibrate the installed flow meters.

**Principle of tracer dilution technique**

The principle of tracer dilution method is illustrated in Fig 1. A known concentration of radiotracer ($C_1$) is injected into a stream (pipeline or canal) at a constant rate *q* over a sufficiently long duration of time. A downstream location is selected for collection of samples at which the tracer is homogeneously mixed known as the mixing distance with the entire cross-section, i.e., the variation of radiotracer concentration across the flow cross-section is less than 0.5 % The concentration of injected tracer is measured at a point beyond the mixing distance and a concentration-time plot is plotted (Fig.1). The region in the curve, where the tracer concentration becomes constant is known as the plateau region. Samples are collected for the measurement of radiotracer concentration after dilution ($C_2$) from a downstream location beyond the mixing distance. The stream flow rate (Q) is computed from Eq. 1 for the conservation of mass as explained below. The background tracer concentration before tracer injection is $C_0$.

$$qC_1 + QC_0 = (q + Q)\, C_2$$

$$\text{Since } Q>>>q,\ q + Q \approx Q$$

$$\text{Also, } C_2>>>C_0$$

$$\text{Therefore, } Q = q \times [C_1/ C_2] \qquad (1)$$

The sampling point at downstream location is critically dependant on the complete mixing of tracer across the cross-section of the flow. The mixing length ($L_m$) depends on the geometric dimension of the channel cross-section, discharge and turbulence levels. The mixing distance for open channel and closed conduit flow can be estimated experimentally as well as theoretically. Several empirical formulae have been reported in the literature for estimation of the mixing distance required for flow rate measurements in open channels [1, 19-22] using tracers and formula gives the most satisfactory estimation of the mixing length (Eq. 2). Similarly, the mixing distance required for closed conduits is determined as per the guidelines specified in the standard ISO 2975, which is about 140 times the pipeline diameter [23, 24]. Rimmar's empirical formula [1, 25] for mixing length ($L_m$) is given by,

$$L_m = \frac{0.13b^2C(0.7C+2\sqrt{g})}{gd} \qquad (2)$$

where, b: mean width of the channel, d: mean depth of the channel, C: Chezy coefficient of roughness ($15<C<50\ m^{1/2}/s$), g: acceleration due to gravity. The above empirical formula (Eq. 2) was used for estimation of mixing length in the case studies described in this article.

There are ways to reduce the mixing length. This is possible by distributed injection, i.e, tracer is injected in several discrete points along the width of the channel. In case of flow measurements in pipelines, if the radiotracer is injected at the suction end of the pump, the mixing will be enhanced, thereby decreasing the mixing length.

The radiotracer should be injected continuously at a particular rate over a sufficient time period to establish an equilibrium concentration at the sampling point and to allow adequate time for collection of a few samples. The injection duration comprises of duration of sample collection and duration of buildup of the plateau (*t*) (Fig. 1). The duration of sample collection is estimated by the total number samples to be collected. In case of a straight measuring length and turbulent flow, *t* can be calculated from Eq (3) [23].

$$t = \frac{6}{u}\sqrt{\frac{Dx}{2}} \qquad (3)$$

where, u: mean velocity of the flow (m/s), x: distance of sampling location from the injection point (m), D: conduit diameter (m).

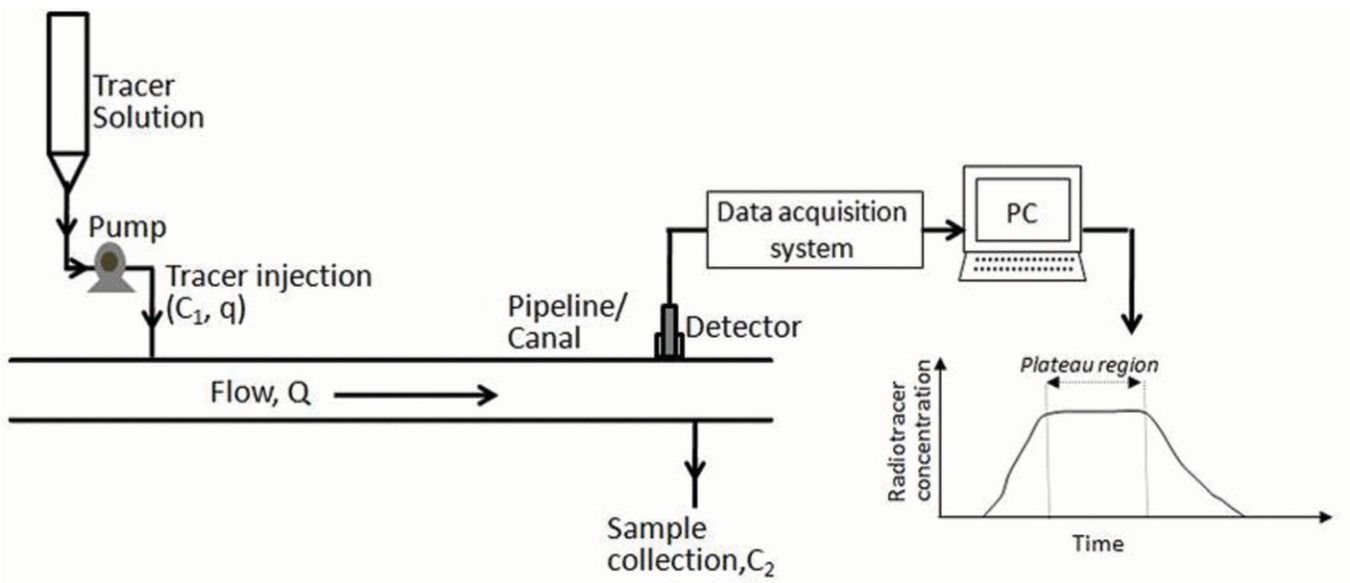


**Fig.1. Principle of tracer dilution technique**

**Radiotracer methodology**

An ideal tracer is a substance that is intentionally introduced into a system, be it biological, industrial or environmental, to study the dynamics of the process material flowing through the system. The tracer quantity should be small and its introduction into the system should not disturb the flow. Further, it should be distinguishable from the process material for its detection. In case of a radiotracer, radioactivity is the property that distinguishes it from the bulk process material and enables its detection. Also, the tracer should not get adsorbed on walls of the system. In case of tracing a phase without any chemical reaction; the radiotracer should have physical properties similar to that of the process material being traced. But if a phase being traced involves a chemical reaction, the radiotracer should have physical and chemical properties identical to that of the phase being traced.

The procedure for flow rate measurement using radiotracer dilution method involves selection of a suitable radiotracer, estimation of amount of activity required for the measurements, preparation and its transport to the experimental site, continuous injection of a known amount of radiotracer at a constant rate, online monitoring of its concentration, sample collection at a downstream location, measurement of concentration in the injected and collected samples; and estimation of the flow rate. Some of the major steps involved are discussed below.

***Selection of radiotracer***

The selection of a radiotracer for a particular study requires careful consideration of various characteristics of the radiotracer such as physico-chemical behaviour, half-life, type and energy of radiation, possibility of production, specific activity and radiotoxicity. In majority of the industrial applications, the phase tracing does not involve a chemical reaction and thus only the physical properties of the radiotracer need to be considered. This enables the selected radiotracer to mix homogeneously within the phase being traced. For '*in situ*' detection, a gamma-emitting radiotracer is selected and the energy of the emitted gamma radiation should be sufficiently high to penetrate through the wall of the system and get detected. Lower energy gamma emitting tracers are, on the other hand, easier to transport in view of their modest shielding requirement. The half-life of the selected radiotracer should be sufficiently long to prepare the radiotracer, transport it to the experimental site and complete the measurements; and at the same time it should be short enough to minimize any environmental hazards. The selected radioisotope used for preparation of the radiotracer should have sufficiently high neutron absorption cross-section to enable its production in desired quantities. Also, the selected radiotracer should have low radiotoxicity. The specific activity of a radiotracer is an important factor to be considered from the radiological safety point of view. One would usually

**Table 1: Commonly used radiotracers used for flow measurements in industry and environment**

| Radioisotope | Half-life | Major gamma energy, MeV (% abundance) | Chemical form | Tracing medium |
|---|---|---|---|---|
| Iodine-131 | 8.04 d | 0.36 (80%)<br>0.64 (9%) | Sodium iodide<br>Potassium iodide | Water |
| Sodium-24 | 15h | 1.37 (100%)<br>2.75 (100%) | Sodium carbonate | Water |
| | | | Sodium salicylate | Organic liquid |
| Bromine-82 | 36 h | 0.55 (70 %)<br>1.31 (27%) | Potassium bromide,<br>Ammonium bromide | Water |
| | | | p-dibromo benzene | Organic liquid |
| Technetium-99m | 6 h | 0.14 (90%) | Sodium pertechnetate | Water |
| Molybdenum-99 | 67 h | 0.18 (4.5%)<br>0.74 (10%)<br>0.78 (4%) | Sodium molybdate | Water |
| Gold-198 | 2.7 d | 0.41 (99%) | Chloroauric acid | Solid (Adsorbed) |
| Lanthanum-140 | 40 h | 1.16 (95%)<br>0.92 (10%)<br>0.82 (27%)<br>2.54 (4%) | Lanthanum Chloride | Solid (Adsorbed) |
| Scandium-46 | 84 d | 0.89 (100%)<br>1.84 (100%) | Scandium oxide | Solid (Particle) |
| Krypton-79 | 35 h | 0.51 (15%) | Krypton | Gas |

transport small volume of the radiotracer to the experimental site as they are easy to shield and manoeuvre. But the injection of high specific activity poses a risk of loss of the tracer on the wall of the system. The probability of such risk is greatly reduced by adding a carrier i.e. non-radioactive counterpart to the injected tracer. The commonly used radiotracers used for flow rate measurements of different phases in industrial and environmental systems are given in Table 1. Based on the above considerations, Iodine-131 as NaI was selected and used as radiotracer in the case studies described in this article.

***Amount of radiotracer***

The amount of radiotracer required to measure flow rate is estimated by considering the detector sensitivity for a specific radioisotope at a chosen detection geometry, accuracy desired, expected dilution between the injection and the measuring location and natural background radiation. The detector sensitivity (counts per unit time per unit volume per unit radioactivity) is estimated in the laboratory prior to the field measurements. To minimize possible loss of radiotracer due to adsorption on different surfaces, a non radioactive carrier (similar chemical properties as the radioactive tracer) is always added to the tracer solution before injection.

Based on the above considerations, about 55 GBq activity of Iodine-131 was estimated to be used for flow rate measurements in the canal. Similarly, the amount of radiotracer required for the flow rate measurements in the pipelines was estimated to be about 11 GBq when only one pump was operated and 22 GBq when two pumps were operated.

***Preparation of radiotracer***

The radiotracer is prepared by neutron irradiation of a suitable target material in a nuclear reactor followed by chemical processing (if required). The target material is chosen in such a way that, it should undergo nuclear reaction with thermal neutrons to produce the desired radiotracer with appreciable yield. The yield of the product radioisotope depends upon amount of starting material, natural abundance of the target isotope and cross-section of the nuclear reaction. Iodine-131 ($^{131}I$) in the form of sodium iodide has been used as radiotracer in the two case studies reported here. Hence the preparation of $^{131}I$ radiotracer is explained below. An accurately weighed tellurium dioxide ($TeO_2$) powder was irradiated in DHRUVA reactor at a thermal neutron flux of $5 \times 10^{13}$ n $cm^2$ $s^1$ for 21 days. After the irradiation, the can was cooled for 2 days and was transported to the radiochemical processing laboratory in a lead shielded flask.$^{131}I$ is produced by $^{130}Te(n,\gamma)^{131}Te$ nuclear reaction ($\sigma_{th}$= 200 mb) followed by beta decay. The $^{131}I$ radioisotope was separated from the target by dry distillation. $^{131}I$ is dissolved in aqueous solution and exist in the form of sodium iodide.

**Case studies**

The radiotracer dilution method was used for flow rate measurements of water in a branch canal of a canal system and large diameter pipelines in a power plant. The two case studies are described below in details.

***Flow rate measurements in a canal***

The Sardar Sarovar Project (SSP) shown in Fig. 2, Gujarat, India, an inter-state and multipurpose river valley project irrigates Gujarat, Rajasthan and Maharashtra, provides drinking water to a large number of villages in Gujarat and generate hydropower. The project consists of a main terminal dam on the river Narmada along with 30 major dams, 135 medium dams and 3000 minor dams, a canal system and two

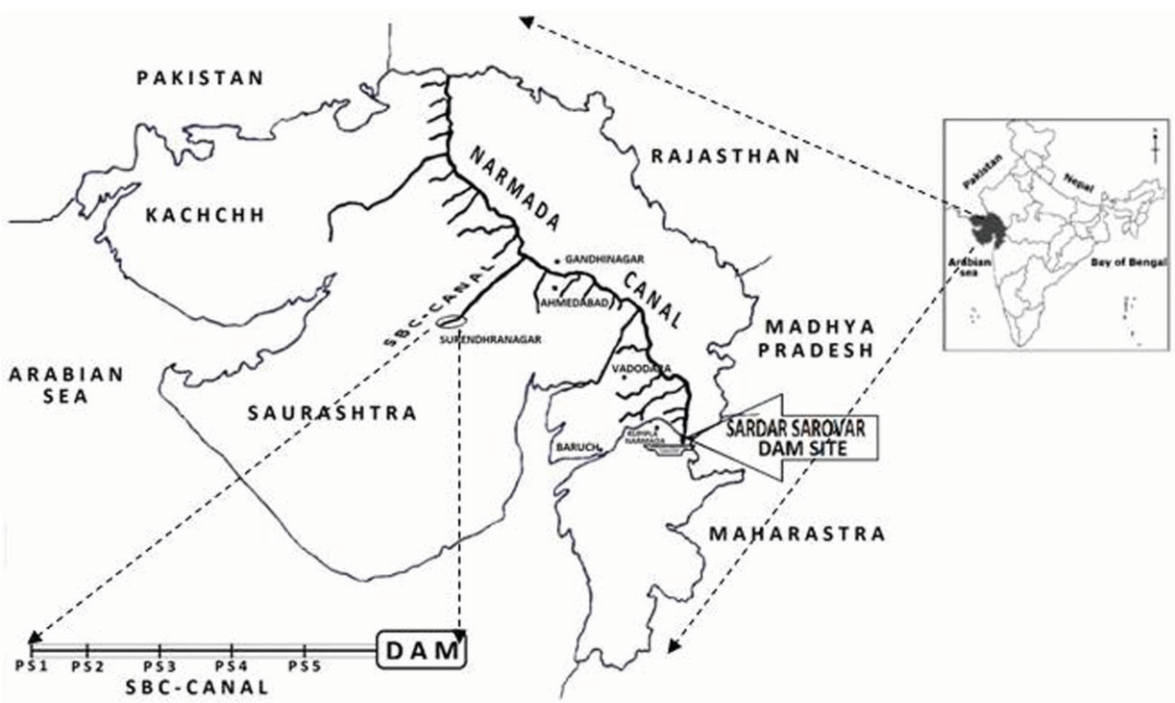


**Fig. 2: Site map and location of the canal**

hydropower stations. The canal system consists of 532 km Narmada Main Canal, with a capacity of 1133 $m^3/s$ at the head regulator 38 branch canals taking off from the main canal, covering a total length of 75,000 km, supply to about 2 million hectares of land. The Saurashtra Branch Canal (SBC) is the largest branch canal of Narmada Canal system, which takes off from the Narmada Canal near the village Karannagar. The SBC is 104 km long and tails into Bhogavo II reservoir (Dholi Dhaja Dam) near Surendranagar (Fig. 2).

For supplying water to Saurashtra and Kachchh regions where natural terrain prevents gravity flow, huge pumping stations have been provided at different locations. On the SBC, the total lift of 71 m is provided by a series of five pumping stations with pumping head ranging from 10.8 m to 17 m. In these pumping stations, a total of 26 Concrete Volute (CV) Pumps each having capacity of 20 $m^3/s$ and 22 Vertical Turbine (VT) Pumps each of 5 $m^3/s$ capacity are installed. After design, engineering, construction and commissioning of all five pumping stations one of the mandatory requirements was to measure discharge rate for validation of efficiency of the installed CV pumps, energy auditing, and effective management and distribution of water.

The radiotracer dilution method was used for measurement of flow rates in four different sections of SBC. Five pumping stations (PS1, PS2, PS3, PS4 and PS5) were constructed along the 104 km long section of the SBC canal and used for pumping water. Fig. 3 shows a typical pumping station used for pumping the water through the canal and the crosssection of the canal. Each pumping station comprises of 5-6 identical CV pumps. The flow rates were measured at four pumping stations PS2, PS3, PS4, and PS5 with single pump in operation at each station.

For each test, the radiotracer solution was prepared by diluting the radiotracer containing 55 GBq activitiy of $^{131}I$ in a volume of 15 litre of water in a graduated cylindrical vessel. About 0.06% inactive potassium iodide and 0.3% of sodium thiosulphate was also added and homogeneously mixed within the solution to minimize the losses due to adsorption and evaporation, respectively. 20 ml of this solution was withdrawn, further diluted to a volume 20 L in three successive steps with a dilution factor of $10^7$ and stored for the measurement of $C_1$. The prepared radiotracer solution was injected at the suction end of the pump at a known constant rate (q) (Table 2) as shown in Fig 4. The injection rate was also manually estimated by monitoring the reduction in volume of tracer solution with time as shown in Fig 5.

**Fig. 4: Injection of radiotracer into suction end of the CV pump**

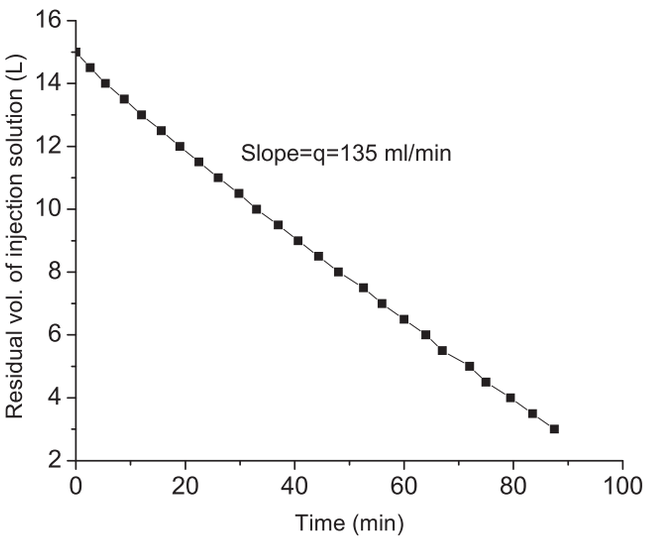


**Fig. 5. Measurement of injection rate of radiotracer**

The samples for measurement of radiotracer concentration ($C_2$) were collected from a downstream location (Fig 3b) at which the radiotracer was expected to mix homogeneously

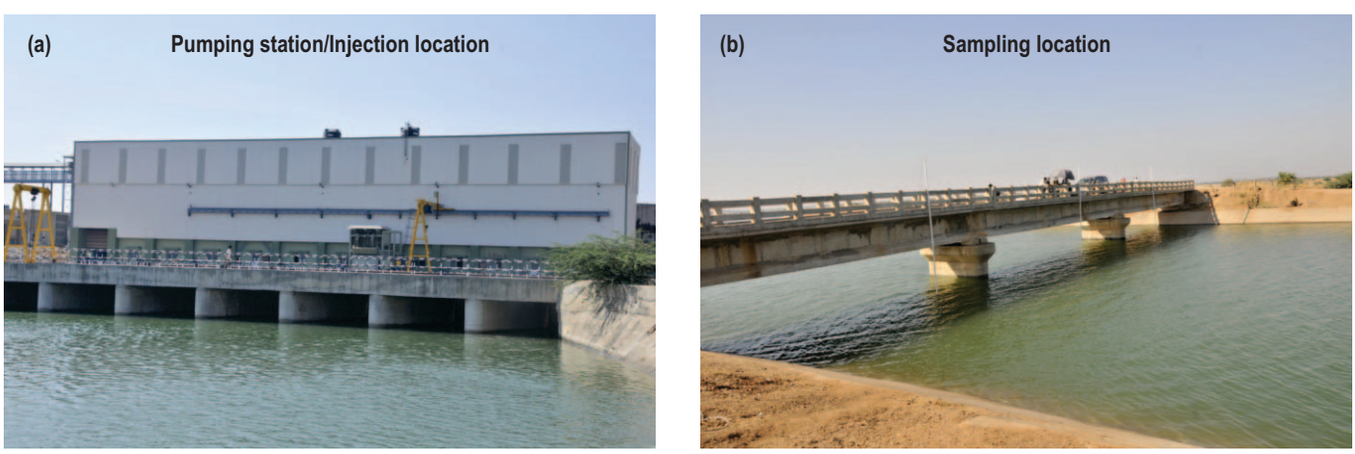


**Fig. 3: Photograph of the canal showing the injection and sampling location**

within the entire cross-section of the canal. For the present case, the mixing length required for the radiotracer to mix homogeneously with the entire cross-section was estimated to be about 405 m.

However, the samples were collected from downstream locations i.e. about 900-2700 m away from injection point. Therefore, sufficient mixing length was provided for radiotracer to mix homogeneously across the cross-section of the canal. The radiotracer concentration in the injected solution ($C_1$), collected samples ($C_2$) was measured using a specially fabricated sampling vessel (20 L) mounted with a NaI(Tl) scintillation detector connected to a data acquisition system. The sampling vessel and the data acquisition are shown in Fig 6 and Fig 7, respectively. The detector was set to record tracer concentration at an interval of 2 minutes during the sample measurement. Identical detection geometry and conditions were maintained during measurement of tracer concentration in injected solution ($C_1$) and samples collected from monitoring locations ($C_2$). Similar experimental procedure was adopted in all four flow measurement tests. The flow rates measured at four pumping stations of the canal with a single CV pump in operation at each station are given in Table 2 and were found to be ranging 20.30±0.29 - 20.62±0.26 $m^3/s$. The measured values of flow rates at four different pumping stations were found to be in good agreement with the theoretically estimated discharge rates of the respective pumps.


**Fig. 6: Setup for off-line measurement of radiotracer concentration**

***Flow rate measurements in large diameter pipelines***

The flow measurements were carried out in two large diameter pipelines in a coal based thermal power plant at M/s Hinduja National Power Corporation Limited (HNPCL), Vishakhapatnam, Andhra Pradesh, India. The plant has two units (Unit-1 and Unit-2) each of 520 MW capacity. Steam produced in the plant is fed into the steam turbine at high pressure and temperature for generation of electric power. The exhausted steam is condensed in condensers and fed back into the boiler for reuse. Sea water is pumped through two different pipelines, each of diameter 3.6 m, using Vertical Turbine (VT) pumps and circulated through the condensers for steam condensation. A typical pipeline is shown in Fig.8.


**Fig. 7. Multi-input data acquisition system (MIDAS) with a NaI(Tl) scintillation detector**

**Table 2: Results of flow rate measurements in the canal**

| Pumping station, PS2 | | | |
|---|---|---|---|
| q (ml/min) | $C_1$ (counts/2 min) | $C_2$ (counts/2 min) | Q ($m^3/s$) |
| 135.00 | $5.662 \times 10^{10}$ | 6275 | 20.30±0.29 |
| Pumping station, PS3 | | | |
| 156.00 | $9.304 \times 10^{10}$ | 11760 | 20.62±0.26 |
| | Pumping station, PS4 | | |
| 143.81 | $2.197 \times 10^{11}$ | 25811 | 20.47±0.22 |
| | Pumping station, PS5 | | |
| 144.07 | $1.0426 \times 10^{11}$ | 12179 | 20.60±0.37 |

Fig. 8: Large diameter pipelines used for transporting the cooling water

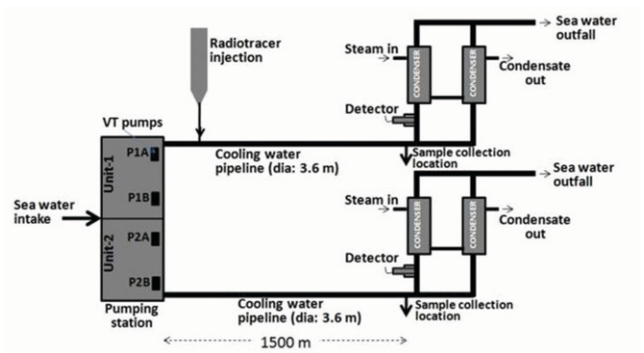


Fig.9: Schematic diagram of the cooling water circulation system and experimental setup for flow rate measurements

A schematic diagram of the experimental system is shown in Fig 9. There are two independent pumping stations for each unit and each pumping station has two identical VT pumps for pumping the sea water for cooling. The pumps, P1A and P1B are used for pumping water in Unit-1, whereas the pumps P2A and P2B are used for pumping the water in Unit-2. Four tests were performed with operations of P1A; P1A and P1B simultaneously; P2A; and P2A and P2B simultaneously for flow rate measurements. The radiotracer stock solution preparation and the tracer injection were carried out in a similar manner as mentioned in previous case study described in the current article. In this case about 11-22 GBq activity of $^{131}I$ was used in each measurement. The radiotracer injection system used for injecting the radiotracer into the pipeline is shown in Fig 10.

An aliquot of 20 ml was collected from the stock solution, further diluted to a volume 20 L in three successive steps with a dilution factor of $10^6$ and stored for measurement of $C_1$. The samples for the measurements of tracer concentration $C_2$ were collected from a downstream location at a distance of 1500 m from the injection point. This distance was sufficient enough for the radiotracer to mix uniformly across the cross-section of the pipe. The concentrations of radiotracer in injected solution and in sample collected at downstream were measured as mentioned in Section 4.1. The results obtained from the flow rate measurements in large diameter pipelines in the thermal power plant are given in Table 3.

Fig.10: Injection system used of injecting the radiotracer into the pipeline

Table 3: Results of flow rate measurements in large diameter pipelines

| Unit-1, P1A | | | |
|---|---|---|---|
| q (ml/min) | $C_1$ (counts/2 min) | $C_2$ (counts/2 min) | Q ($m^3$/s) |
| 188.2 | 5.867 x $10^{10}$ | 11875 | 15.43±0.46 |
| Unit-1, P1A+P1B | | | |
| 187.2 | 3.755 x $10^{10}$ | 4240 | 27.51±0.82 |
| Unit-2, P2A | | | |
| 220.8 | 3.096 x $10^{10}$ | 8044 | 14.10±0.43 |
| Unit-2, P2A+P2B | | | |
| 185.1 | 6.626 x $10^{10}$ | 8291 | 24.55±0.78 |

The values of the flow rates of cooling water in the pipelines of Unit-1 and Unit-2 of the power plant were measured to be 15.43±0.46 and 14.10±0.43 $m^3$/s, respectively when only one VT pump was operated in each unit. Whereas, the values of the measured flow rates were found to be 27.51±0.82 and 24.55±0.78 $m^3$/s, respectively when both the pumps were operated simultaneously in each unit. To the best of author's knowledge the flow rate measurement in such large diameter pipelines using radiotracer dilution technique has been carried out for the first time.

**Radiological safety**

The radiotracer tests were carried out by trained and authorized personnel of Isotope and Radiation Application Division (IRAD), Bhabha Atomic Research Centre, Mumbai

with prior approval Atomic Energy Regulatory Board (AERB). The radioactive waste generated was stored in a suitable container and placed in an isolated room to allow the activity to decay before disposal. The general guidelines for safe handling and use of radioisotopes issued by International Commission on Radiological Protection (ICRP) and AERB were followed during the investigations. In current investigation, the injected radiotracer was diluted in large volume of water and the concentration of Iodine-131 in the water was much below than the prescribed limit. Therefore, the injected radiotracer did not pose any radiation hazardous to the public and environment.

**Conclusions**

The radiotracer dilution technique was developed, standardized and successfully applied for measurements of water flow rate in two large-scale industrial systems i.e. canal and large-diameter pipelines. The values of the flow rates measured in the two systems were found to be in good agreement with the theoretically estimated values of the respective pumps. This lead to the conclusion that both types of pumps behaved as per the design criteria. The flow rate measured in the SBC canal at M/s SSNNL, Surendranagar, Gujarat, were used to optimize the pumping operation, water distribution through various branch canals and energy consumption and; water budgeting.

In case of flow rate measurements in large diameter pipelines at M/s HPNCL, Vishakhapatnam, Andhra Pradesh, the values of the flow rates measured by the installed flow meters were found to be significantly different from that of the values measured using radiotracer dilution technique. This implied that either the calibrations of the installed flow meters were altered during the operation or the flow meters were malfunctioning. Subsequent to the flow rate measurements using radiotracer dilution technique, the installed flow meters were uninstalled and found to be malfunctioning. The flow meters were repaired, recalibrated and installed back on the pipelines. After the reinstallation of the flow meters, the values measured by the flow meters were found to be in good agreement with the values measured using the radiotracer dilution technique.

The application of the radiotracer dilution technique helped, to validate the efficacy of the two different types of the pumps, to calibrate the installed flow meters, optimize the pumping operation and water distribution leading to significant economic benefits to both the industries. The technique proved to be sensitive and versatile for flow measurements; and can be applied for accurate measurement of flow rates in systems were conventional methods cannot be used.

**Acknowledgments**

The authors wish to thank the authorities of M/s Kirloskar Brothers Limited, Pune; M/s Sardar Sarovar Narmada Nigam Limited (SSNNL), Surendranagar, Gujarat and M/s Hinduja National Power Corporation, Visakhapatnam, Andhra Pradesh for providing necessary logistic support and help in conducting the flow rate measurements.

**References**

1. Rimmar, G. M, 1960. Use of electrical conductivity for measuring discharges by the dilution method, National Engineering Laboratory Translation No.749, Trudy GGI, 36 (90), 18-48.
2. United State Geological Survey, 1965. Measurement of discharge by dye-dilution techniques, Chap. 14, Surface Water Techniques, USGS, Washington DC.
3. British Standards Institution, 1974. Methods of measurement of liquid flow in open channels: Part 2, Dilution methods; 2A, Constant-rate injection, BS 3680; Part 2A, London.
4. International Organization for Standardization, 1983. Measurement of Liquid Flow in Open Channels, ISO Standards Handbook 16, ISBN 9267100777, Geneva, Switzerland.
5. Kilpatrick, F.A. and Cobb, E.D., 1985. Book 3, Chapter Al6, Measurement of Discharge Using Tracers, The United States Geological Survey, Washington.
6. Benischke, R. and Harum, T., 1990. Determination of discharge rates in turbulent streams by salt tracer dilution applying a microcomputer system. Comparison with current meter measurements, Hydrology in Mountainous Regions. I - Hydrological Measurements; the Water Cycle, IAHS Publ. no. 193, Wallingford
7. World Meteorological Organization, 2010. Manual on Stream Gauging, Volume I– Fieldwork WMO-No. 1044, WMO, Geneva, Switzerland.
8. Muthukumar, U., Chandapillai, J., Saseendran, S., 2010, Flow measurement in hydroelectric stations using tracer dilution method – case studies , IGHEM-2010, Oct. 21-23, 2010, AHEC, IIT Roorkee, India.
9. Liptak, Bela G., Flow Measurement, 1993. CRC Press.
10. International Atomic Energy Agency, 1990. Guidebook on radioisotope tracers in industry. IAEA, Vienna (Technical Report Series No. 316), pp.374.
11. International Organization for Standardization, 1994. Measurements of liquid flow in open channel - Tracer dilution methods for the measurement of steady flow - Part 1, ISO 9555-1, Geneva, Switzerland.
12. Charlton, J. S., 1986. Radioisotope Tracer techniques for problem solving in industrial plants. Leonard Hill, Glasgow and London, pp.320.
13. Smart, P.L. and Laidlaw, I.M.S. 1977. An evaluation of some fluorescent dyes for water tracing, Wat. Resour. Res. 13, 15-33.

14. Smith, D.B., 1964. River flow Measurement using Radioactive Tracers. Dilution Techniques for Flow Measurement, Bulletin, No. 31. Paper 8, Dept. of Civil Engineering, Univ. of Newcastle, Newcastle, New South Wales, Australia.
15. British Standards Institution (1967) Methods of measurement of liquid flow in open channels. Part 2. Dilution methods. 2C. Radioisotope techniques. BS 3680 Part 2C, London.
16. International Atomic Energy Agency, 1968. Guidebook on nuclear techniques in hydrology. Tech.Rep.Ser.No.91, IAEA, Vienna.
17. International Organization for Standardization, 1973. Liquid Flow Measurement in Open Chnnnels-Dilution Methods for Measurement of Steady Flow-Constant Rate Injection Method", ISO Standard 555/1.
18. International Organization for Standardization, 1974. Liquid flow measurement in open channels-dilution methods for measurement of steady flow-integration (sudden injection) method. ISO Standard 555/11.
19. Elder, J.W. 1959. The dispersion of a marked fluid in turbulent shear flow. Journal of Fluid Mechanics 5(4): 544–560.
20. Hull, D.E., Dispersion and persistence of tracer in river flow measurements, 1962. Int. J. App. Rad. and Isotopes, 13.
21. Barsby, A., 1968, Determination of mixing length in dilution gauging, International Association of scientific hydrology publication no. 78, 395 - 407.
22. Ward, P. R. B., 1973. Prediction of mixing lengths for river flow gauging, J. Hydraul. Div. Am. Soc. Civ. Eng., 99(7), 1069– 1081.
23. International Standards Organization, ISO 2975-3:1976, Measurement of water flows in closed conduits-tracer methods-Part III, Constant rate injection method using radioactive tracers, Geneva, 1976.
24. Proceedings of the symposium on Radioisotope Tracers in Industry and Geophysics, Prague, 21 - 25 November, 1966. Printed by International Atomic Energy Agency, pp 564.
25. Subramanya, K., Engineering Hydrology, 1994, pp 115.

# Development of External Pipeline Inspection Gauge for Monitoring the Health of Industrial Carbon Steel Pipelines

**Shilpi Saha, S.C. Ramrane, D. Mukherjee, Y. Chandra, S.K. Lahiri and P.P. Marathe**
Control Instrumentation Division

**A.C. Bagchi**
Integrated Fuel Fabrication Facility

BARC has developed a fleet of Instrumented Pipeline Inspection Gauges (IPIGs) for health monitoring of buried carbon-steel pipelines carrying petroleum product. These tools, once inserted into the pipeline, travel with the cargo without disturbing the throughput and record MFL signals emanating from the pipe surface. However, there are pipelines in oil refineries, process industries and power plants (conventional and nuclear) where inspection from inside is not possible/ (which are unpiggable from inside). These lines are mostly inspected at few locations during in-service inspection schedule, but full periphery and full length inspection coverage is not feasible due to the unavailability of any standard inspection tool. Nevertheless, integrity management of such pipes are of paramount importance. A novel inspection tool known as External PIG (EPIG) has been developed for 6" NB liquid waste discharge pipeline of IF3. The tool inspected the line and produced encouraging results. The results have been verified independently at several locations. The tool is light weight, easy to handle and can do quick inspection of the pipeline from outside. This paper outlines the development work of EPIG from inception to field trials with inspection results.

## Introduction

Over the years, BARC has developed a fleet of in-line-inspection (ILI) tools ranging from 12" to 24" for in-line inspection of buried oil pipelines. These tools are now commercially available in the country and are being extensively used for health monitoring of cross country pipelines of IOCL and other PSUs. Using the expertise and domain knowledge in the area of in-line inspection, a magnetic flux leakage (MFL) based External pipeline inspection gauge (EPIG) has been developed for inspection of 6" pipeline of IF3, BARC. The tool inspects the pipeline externally for both near wall (external surface) and far wall (internal surface) defects. These pipelines are usually inspected at specific locations, but are never inspected for full length with 100% peripheral coverage due the lack of standard inspection tool or available methodology. Recently, research has been directed towards this area with an attempt to build automated robots with magnetic wheels to scan pipe surface externally [1]. The tool scans a small sector of a large diameter pipeline, while moving autonomously over the pipe surface. Similar non-autonomous tools with spot classification capability (go/no-go) and much lower sensitivity are also available commercially [2]. However, none of the developments point towards a comprehensive full-periphery pipeline inspection technique and defect characterization methodology.

In the present development, a tool, split in two halves, is designed to scan the full periphery of the pipe externally. In the presence of a corrosion (metal loss) defect, the leakage flux near the defect will increase and in turn is sensed by a series of hall-effect sensors spanning the full-periphery. The signal is observed in near real-time as well as stored for offline analysis.

## EPIG development

### *Basic Principle*

MFL signals are widely used for non-destructive evaluation (NDE) of defects in carbon steel petroleum cross-country buried pipelines. The principle involves magnetizing a section of pipe to near saturation and sensing the leakage flux at the magnetic neutral plane with hall-effect sensors. In presence of corrosion defect or gouging or any other pipeline feature, e.g. welds, flanges etc the leakage flux signature would change, indicating the presence of anomaly [3].

### Tool development

The EPIG tool contains magnetizer, sensors, support rollers and odometers. Acquisition cum processing electronics and power supplies are housed in a separate casing outside the tool. The design of the tool has evolved iteratively through Finite Element (FE) modelling to optimize the magnetic saturation level inside the pipe. Challenge of the design was to ensure ease of tool handling while maintaining uniform magnetization level around full-periphery of pipe. Fig. 1 shows magnetization baseline inside the pipe for two such design trials, (a) a three module magnetizer and (b) a four module magnetizer. It shows that four module design yields more uniform magnetic field of higher strength and hence, it is adopted for final tool design. The complete FEM simulation of the 4 module tool is shown in Fig. 2 The pipe section between pole faces as shown in the Fig. 2 indicates the uniformly magnetised inspection area. A defect of known dimension (a full periphery slot of known depth and length) is made at the centre of this inspection region, and expected leakage flux profile is estimated at various lift-offs from the pipe surface. This gives an estimate of the leakage flux expected to be measured by sensors at various lift-offs. Effective design needs to ensure that any component in the magnetic circuit should not go into deep saturation. The flux level at various locations on the pipe surface as well as on the magnetiser is also noted. This helps in finalizing the mechanical dimensions of the magnetizer unit.

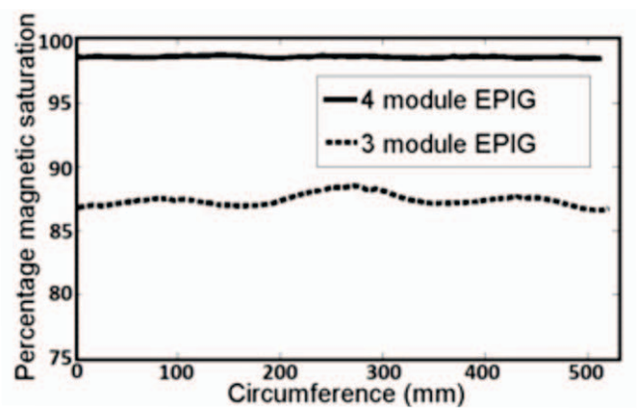


**Fig. 1: Plot showing baseline magnetization level**

The EPIG tool is pulled over the pipe surface at a desired speed by a battery operated winching mechanism. Data is acquired with a desired sampling rate using hybrid sensing system with radial and axial MFL sensor arrays. Signals from these sensors are acquired and recorded by an in-house developed multi-channel data acquisition system (DAS). The system connects to a laptop for a near real-time viewing of the processed sensor data as well as its storage for offline analysis. Odometer system provides accurate localization of any pipe feature or corrosion defect that may get detected.

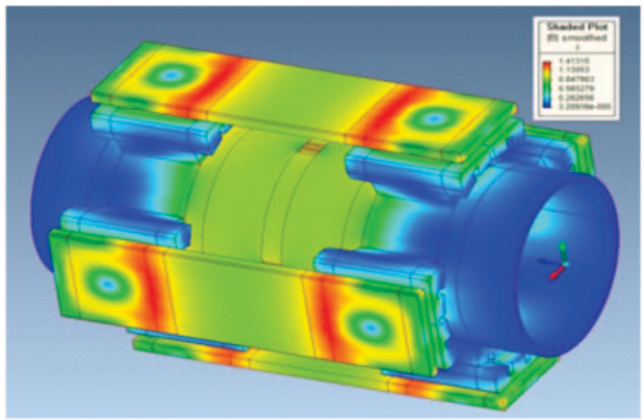

**Fig. 2: FEM simulation of a prototype EPIG design**

### Defect characterisation

Defect templates with known sizes of faults were created on a 1 meter pipe spool and signals were recorded and analysed for generating data-bank. Fig. 3 shows the radial MFL signal recorded from a template defect by an array of sensors passing over it. The data-bank thus generated from these tests, were used to extract MFL signal parameters. As shown in the zoomed images in Fig. 3 the signal parameters extracted are (a) span measured in number of samples, (b) numbers of sensors sensing the defect (estimated from circumferential flux profile) and (c) maximum peak to peak leakage flux recorded by the centremost sensor. These signal parameters are then mapped to defect parameters using an empirical model. More details on signal parameter extraction can be found in [4]. An empirical model is trained based on template data and used for mapping the signal parameters to defect parameters (length, width, %WL).

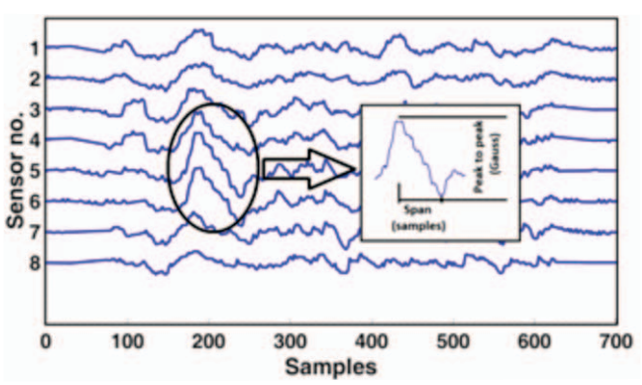


**Fig. 3: Signals obtained from a standard defect (Set 1) over 1 m long pipe**

**Inspection of liquid waste discharge pipeline at IF3, results and validation**

The tool was deployed in field to inspect 6" liquid waste discharge pipeline of IF3, BARC. The complete tool with its sensor arrangement and winching mechanism is shown in Fig. 4 and Fig. 5 respectively.

Fig. 4: EPIG over the discharge pipeline at IF3 BARC

Fig. 5: EPIG tool with its winching arrangement

A total of 59 spools of the pipeline were inspected on a spool by spool basis. The entire inspection took 2 days to complete, with an average of 7-8 minutes inspection time per spool. The total length of inspection is about 250 meter. The schematic map of the inspection area is shown in Fig. 6. The only limitation of the EPIG tool is that it cannot inspect the pipe section at support locations. The tool is dismantled at supports and is again re-assembled for inspection of the next section. However, downtime is only of the order of few minutes (typically 4 – 5 min). The signals from MFL sensors over each spool is observed in near-real time and recorded for further offline analysis. The data recorded from each spool is converted into an image of the pipe surface (C-scan). The C-scan is generated after de-noising the signal using discrete wavelet transform with thresholding [3]. Such a C-scan can be seen in Fig. 7 . A weld and a metal loss (corrosion) defect (very close to the weld in the upper section) are clearly seen in this image. These are reported, along with its location from the start of the spool. For each metal loss defect, the feature parameters are extracted as explained in Section 2.3 for estimating the defect sizes (length, width and percentage wall-loss).

Based on the report, few severe defects are chosen for site verification. These defects are visually verified (if they are external) and sized with vernier depth gauge measurement or measured with an ultrasonic thickness gauge (for internal defects). From the field run of EPIG, estimated dimensions (length, width and percentage wall loss) of 5 defects were successfully verified on site (including one internal defect).

Three external defects along with their C-scans can be seen in Fig. 7 (one) and Fig. 8 (two). One internal defect can be seen in Fig. 9 (upper section, right of the weld). Defects were found at the precise location estimated by odometer data. The estimated defect parameters and its site-verified measurements are given in Table 1 along with their percentage error. The defects 1 through 4 are external and verified by vernier measurement and 5th defect is internal, and is verified by ultrasonic gauge.

The error observed is well within acceptable limits as per Pipeline Operators Forum (POF) requirements. The site

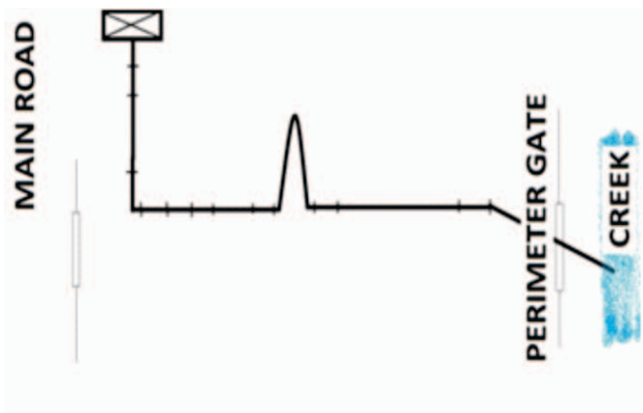


Fig. 6: Map of the liquid waste discharge pipeline inspected at IF3

verification of reported results builds good confidence in overall inspection capability of EPIG. The out of bound errors observed can be reduced further with multiple field trials and by employing more accurate site defect verification gauges.

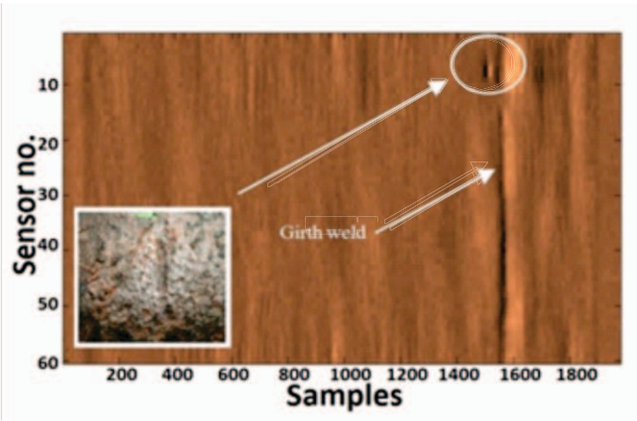


Fig. 7: Corrosion signal along with its actual site verified defect and a girth weld

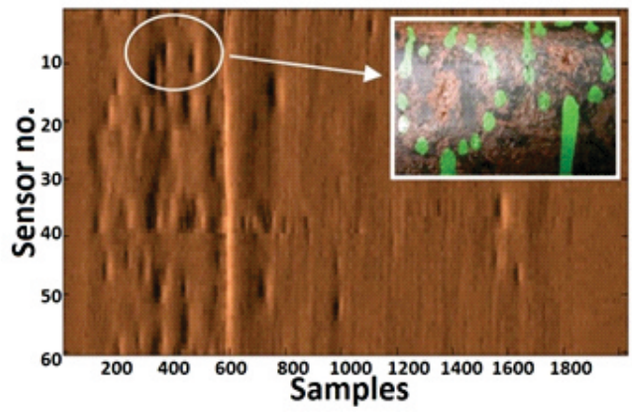


Fig. 8: Corrosion signal along with its actual site verified defect and a girth weld

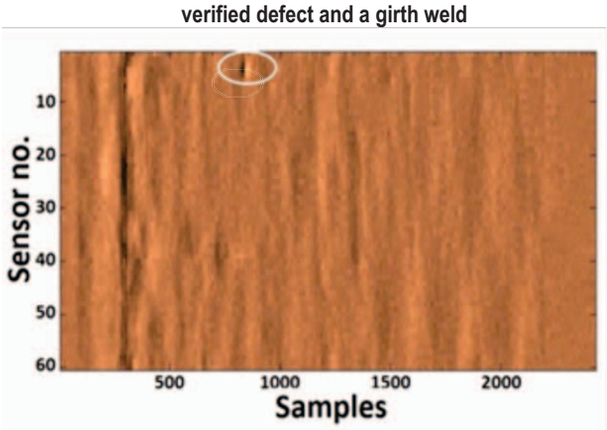


Fig. 9: Internal corrosion defect verified by ultrasonic depth gauge and a girth weld

Table 1: True defect sizes vs defect sizes estimated from EPIG signal

| Sl. No | Parameters (Length (in mm),Width (in mm), %Wall loss) | | |
|---|---|---|---|
| | Estimated | Actual measured | Error(L,W, %wl) |
| 1 | 24,22,28 | 21,23,24 | 3mm, 1mm, 4% |
| 2 | 22,24,22 | 16,26,24 | 6mm, 2mm, 2% |
| 3 | 23,33,20 | 22,31,22 | 1mm, 2mm, 2% |
| 4 | 34,28,21 | 30,20,21 | 4mm, 8mm, 0% |
| 5 | 41,23,22 | 40,40,20 | 1mm, 17mm, 2% |

## Conclusion

The EPIG is a prospective tool for the inspection of carbon steel pipelines from outside. It gives almost full length and full periphery inspection coverage as compared to spot inspection with conventional technique. The ease of assembly and dismantling of the EPIG gives it the necessary advantage to inspect even physically inaccessible areas of pipeline. The tool can be used with minimum modifications to inspect carbon steel pipelines of different sizes existing in various plants and facilities in BARC and other DAE units.

## Acknowledgement

The authors are grateful to Shri D. Das, AD (E), E&IG for his encouragement and support in pursuing specialised NDT applications being developed for BARC and other DAE units. The authors are thankful to Shri V K Gautam and his team from IF3 for their extensive support during inspection trial and site verification of the tool. Special thanks are also due to the South Gate Security personnel for facilitating access to the inspection area during several trial runs.

## References

1. Yukawa T., Suzuki M., Satoh Y., & Okano H. (2006). Design of magnetic wheels in pipe inspection robot. Systems,Man and Cybernetics. Taipei: IEEE International Conference.
2. SILVERWING. (n.d.). Retrieved from www.silverwingndt.com/magnetic-fluxleakage/pipescan-pipe-corrosion-detection
3. Mukherjee D., Saha S., Lahiri S. K., & Mukhopadhyay S. (2014). Application of wavelets in non-stationary signal processing. Third National Symposium on Advances in Control and Instrumentation (SACI). Mumbai.
4. Saha S., Mukhopadhyay S., Mahapatra U., Bhattacharya S., & Srivastava G. P. (2010). Empirical structure for characterization of metal loss defects from radial magnetic flux leakage signal. NDT & E International, Elsevier Science ((43) 507-512), 507-512.

# A Table Top Static Gas Sensing Unit: Model No. TPD-BARC-16CH

**Niranjan Ramgir, R. Datta, K. Avhad, R. Bhusari, M.M. Vedpathak, M. Meera, V.V. Katke, E. Ravisankar, A.K. Debnath, T.K. Saha, K.P. Muthe and S.C. Gadkari**
Technical Physics Division

Table Top Static Gas Sensing Unit (Model: TPD-BARC-16CH) has been designed and developed. This unit is suitable for monitoring or recording the response of 16 sensing elements simultaneously under controlled conditions of operating temperature and gas environment. The indigenous software has also been developed that interfaces the instrument to a personal computer or Laptop. Moreover, the resistance of the sensing elements under investigations is recorded and displayed as a function of time. The unit can measure the resistance variation from 1 G to 1 K or 1 M to 1 . The developed product is unique and no such similar product is available in the market. Importantly, the instrument is useful for the measurement of response curves of chemiresistive sensors.

Keywords: Multiple Sensors Testing Unit, Gas Sensors, Operating Temperature, Data Acquisition

## Introduction

Gas sensing is one of the most widely investigated activities of the materials research [1]. With the advent of nanoscience and nanotechnology novel materials with superior performances are being routinely synthesized [2]. Development of gas sensors based on these materials demands a thorough investigation of these materials under controlled conditions of operating temperature and gas environment [3-4]. Further, to speed up the time for process optimization, simultaneous measurement of multiple sensors under identical conditions is desired but it often requires a very long time. In order to speed up the parameter optimization e.g. sensitizer, its concentration and annealing schedule, it is essential to have a system possessing the capability of recording the response curves under identical conditions of operating temperature and gas environment. To address this need, Technical Physics Division (TPD) has developed a Table Top Static Gas Sensing Unit (Model: TPD-BARC-16CH), which can monitor the responses of 16 sensing element simultaneously. The developed unit is suitable for monitoring or recording the response under controlled conditions of operating temperature and gas environment. Some of the salient features of this product are;

**Technical Specifications of the unit**

| | |
|---|---|
| **Unit: TPD-BARC-16CH**<br>• Input requirement<br>• Weight | <br>230 V, 50 Hz AC<br>Light weight (<2 kg), portable |
| **Test Chamber 1:**<br>• Material<br>• Housing diameter<br>• Housing length<br>• Sensor types | <br>SS-304<br>28 mm<br>50 mm<br>Array |
| **Test Chamber 2**<br>• Material<br>• Housing diameter<br>• Housing length<br>• Sensor types | <br>SS-304<br>81 mm<br>48 mm<br>Individual |
| **Technical Parameters:**<br>• Resistance range<br>• Operating temperature range<br>• Control Software<br>• Acquisition type<br>• Data acquisition mode and speed | <br>MΩ to Ω or GΩ to kΩ<br>RT to 300 ± 2°C<br>Arduino IDE compatible with Labview<br>Simultaneous<br>Adjustable, maximum 4 points/sec |

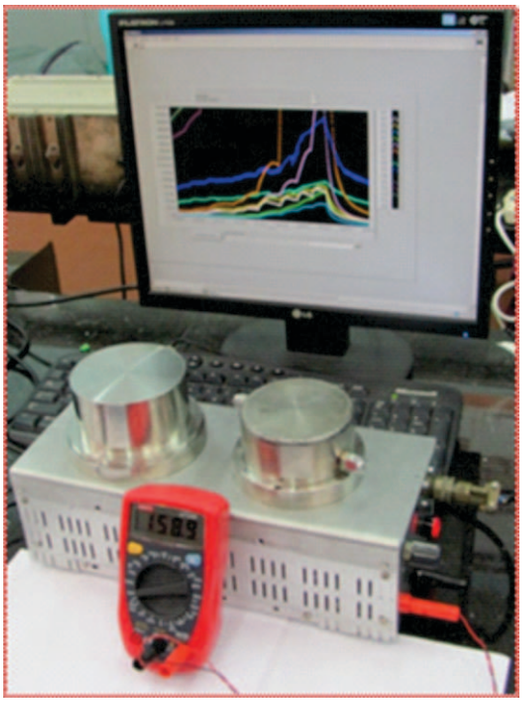

Fig. 1: Table Top Static Gas Sensing Unit, Model No. TPD-BARC-16CH.

- Uniquely positioned product: No such unit in the market is available containing both data acquisition and testing facility in one unit.
- Light weight and portable.
- Six order changes in the resistance can be measured (G - K).
- Two separate test chambers for multiple sensor array (10-16 numbers) and individual sensing element (maximum 7 numbers) testing, respectively.
- Operating temperatures can be tuned in the range from room temperature (RT) to 300oC.
- Real time monitoring with direct interface to personal computer or Laptop.
- Indigenous software, provision to select and deselect the sensing element.

The unit essentially comprises of the following two parts:

- Sensor test chambers and
- Data acquisition unit

**Sensor test chambers**

As shown in figure 1, the unit is equipped with two test chambers containing heaters and readers. The heater temperatures are controlled using potentiometer on the temperature control circuit in the housing below test chambers.

***Test chamber 1***

In this, two sensor arrays comprising of 5 sensing elements each with two heaters and two readers are

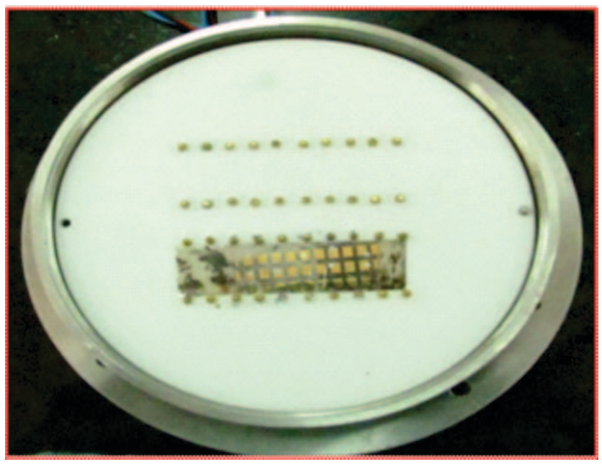

Fig. 2: Teflon disc in the test chamber 1 showing the electrical feed-through for heater, reader and sensing element connection.

provided. It consists of a Teflon disc containing an array (20 x 2) of gas tight electrical feed-through with a spacing of 1.5 cm (figure 2). For measurement of resistance of a sensor array of dimensions 1.5 cm x 3 cm, it is advised to connect heaters at the two edges along with readers. Heaters are made by connecting two Pt-100's in parallel to each other, while reader is just a single Pt-100 whose resistance value as measured using digital multimeter is an indicator for the operating temperature.

The rest of the feed-throughs are connected to the data acquisition card located in the housing below.

***Test Chamber 2***

It consists of seven Teflon heads fixed in stainless steel (SS 304) disc as shown in figure 3 (a). The Teflon heads are provided with 6 pins (phosphor bronze) for electrical connections. Out of these 6 pins, two are used for sensing element, two for the connection of heater and the rest two for the reader as shown in figure 3 (b). The heater wires are connected to the temperature control circuit, reader wires to the 8-pin band change switch and the two sensing element wires to the data acquisition card. Here also, the heater is realized by connecting two Pt-100's in parallel. The heater and the reader Pt-100's are physically connected adjacent to each other so as to form a platform on which the sensing element can conveniently be rested. The heater and reader wires are connected to the phosphor bronze pins in such a way that a direct contact with the Teflon base is avoided.

Figure 4 shows the photograph of the wiring behind the test chambers. Herein color code has been followed, red color wires are used for heater, orange for reader and other colors for the sensing element. As is evident all the heater and reader are routed to the temperature control circuit and the 8-pin band change switch (digital

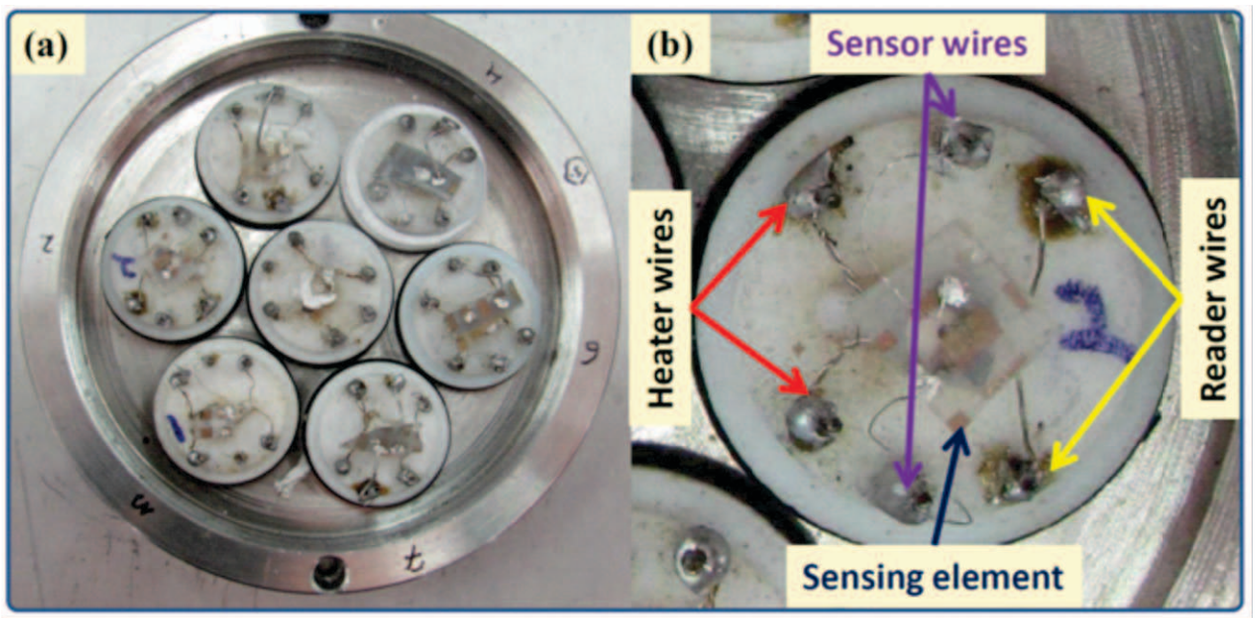


**Fig. 3: (a) Photograph of Test chamber 2 with 7 Teflon heads containing heater, reader and sensing elements, (b) Photograph of single Teflon head showing the connections made to sensing element, heater and reader.**

multimeter) via a general purpose printed circuit board (PCB).

The stainless steel test chambers are provided with two values (inlet and/or outlet). The test volume of the chambers is 250 sccm (standard cubic centimeter). By injecting the known amount of test gas in the chamber through an inlet value provided with septum the concentration of the test gas can be controlled. For recovery measurements, the sensor chamber cap or top needs to be opened subjecting the sensors to the ambient environment. Importantly, the test chambers can be customized to specific needs of the user. Two pairs of either test chamber 1 or 2 can be used with necessary modifications of the wiring or connections.

### Operation of the Instrument

Figure 5 shows the Home screen with various fields. There are three main tabs Data Acquisition (DAQ), settings and retrieval. There are 16 channels (0-15) displaying the resistance values (in k ) of the 16 sensing elements. The color of each channel is different and hence can be used to locate the channel on the screen. The individual sensing element can be selected or

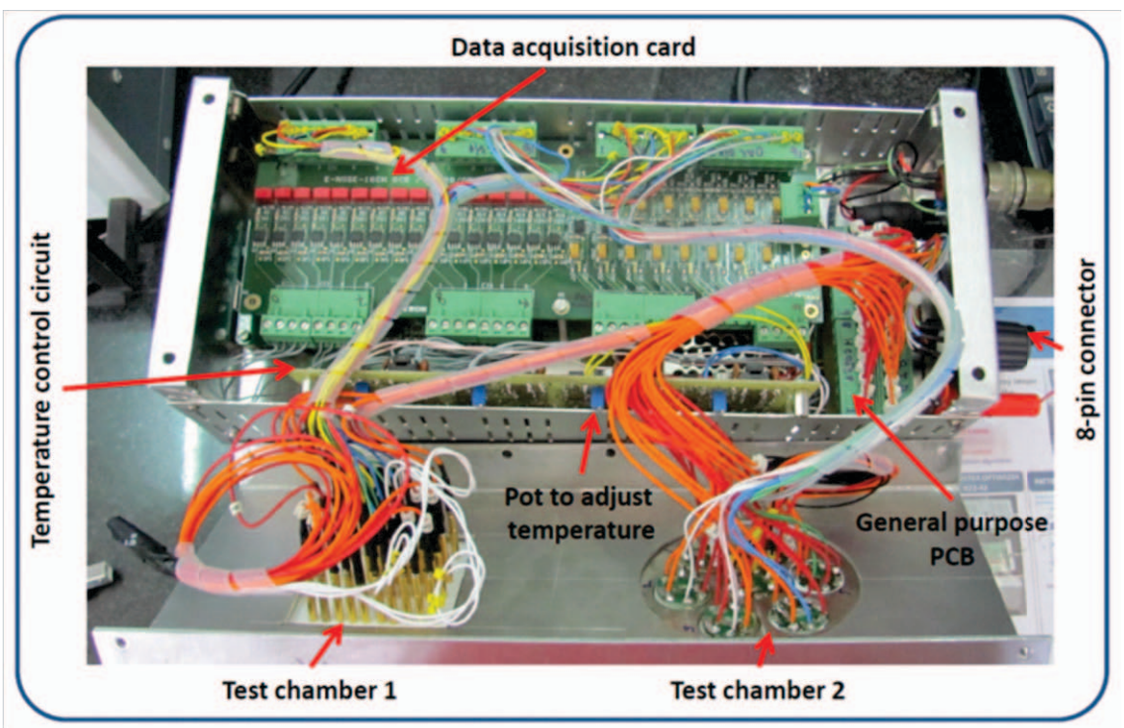


**Fig. 4: Inside view of the unit showing connections or wiring between different components of the unit.**

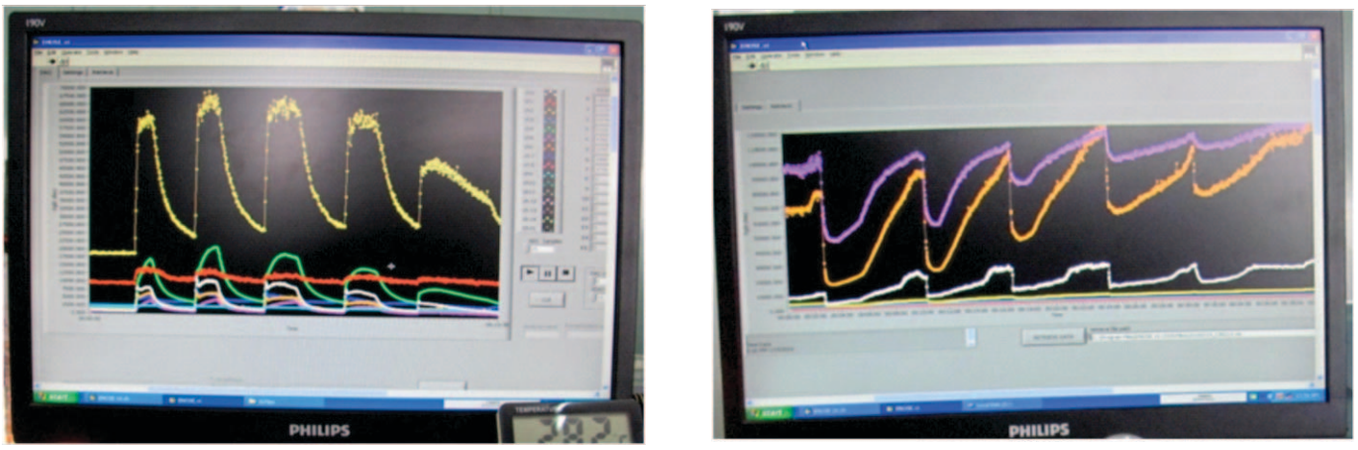


(a) (b)

**Fig. 5: The real time response curves recorded using the unit for the n-type metal oxide sensors upon exposure to (a) oxidizing ($NO_2$) and (b) reducing gas ($H_2S$), respectively.**

deselected as per the requirement in the channel selector. In the settings, tabs options are provided to control or calibrate the data acquisition values (resistance) by setting the multiplication factor (x factor). By default it is set at 1.39. It is also possible to control the data acquisition speed by setting the Analogue to digital Converter (ADC) values.

By default it is set at 30, it can be brought down to increase the data acquisition speed. The retrieval window is also provided to retrieve the previously saved data for comparison or reference, as and when required. The files can be recalled by pressing the retrieve data knob and locating the files through drop down menu.

**Measurement of Response Curves**

Once the sensors are mounted and the operating temperature is fixed, the chamber is closed and a settling time of 15 min is provided. Now, the known concentration of the test gas is injected using an air-tight syringe in the test chamber and the variation in the resistance as a function of time is recorded and monitored. Upon injection of the test gas, the resistance of the sensing element will increase or decrease depending upon the sensing element and the nature of test gas. For example, for n-type metal oxides like $SnO_2$, ZnO, and $TiO_2$ the resistance will decrease or increase when exposed to reducing ($H_2S$, $NH_3$) or oxidizing gases ($NO_2$, $CO_2$), respectively (Figure 5 (a) and (b)). Opposite is the case with p-type materials i.e. with holes as majority carriers. By default the files are saved as ".xls" file (excel) with the name as date and time of measurement. With columns showing the different channels and the rows depicting the resistance values. The first column is the time displayed in seconds. Moreover, the files can easily be accessed and transferred or copied to the other software as per the user requirement.

In order to demonstrate the working of the instrument a multiple sensor array (MSA, 12 sensing elements) based on ZnO nanowires has been tested for its response towards different gases and the results are shown in figure 6. For this ZnO nanowires were deposited using a

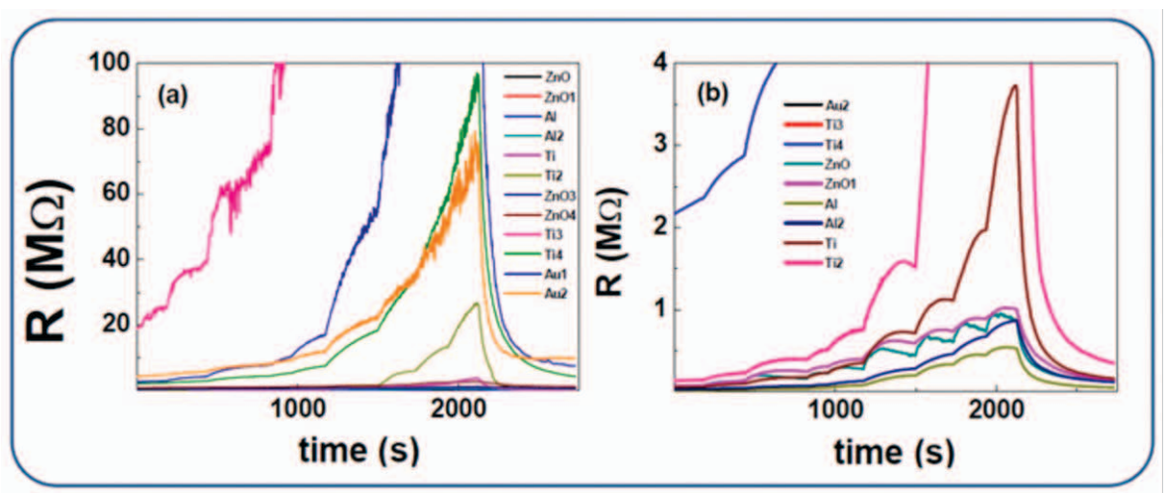


**Fig. 6: (a) Variation of resistances of the MSA upon exposure to increasing concentration of $NO_2$ and (b) Zoomed response curve for the sensing element with smaller response values.**

hydrothermal method [3] and an array of (4 x 3) sensor films were realized by modifying the nanowire film with sensitizers namely Al, Ti, and Au layer. Figure 6 shows the response curves of all the 12 sensing elements towards increasing concentration of $NO_2$ between 1 and 50 ppm. The data was acquired using the instrument and plotted using the origin software.

As shown in figure 6, the 12 sensing elements were tested under identical conditions and accordingly it becomes easier to compare the response curves and the related parameters namely response time, recovery time, sensor response values in a single run. This implies that in a single exposure, it is possible to generate more information that can be used to tune the parameters to realize a better sensing material. Thus the result clearly demonstrates that the present system is capable of speeding up the parameter optimization in order to achieve the required sensing characteristics.

**Conclusion**

A uniquely versatile import substitute product namely a table top static gas sensing unit has been successfully developed, tested and implemented for addressing needs of a client base comprising of universities and other Research & Development institutes. The developed system can record response curves from the 16 sensing elements simultaneously. Two independent test chambers, one for the sensor array and the other for the individual sensing element have been provided. The operating temperature can be tuned right from RT to 300°C. The unit can measure the six order change in resistance from 1 GΩ to 1 KΩ or 1 MΩ to 1 Ω. Importantly, the product demonstrated its utility in speeding up the parameter optimization to achieve required sensing characteristics.

**Acknowledgements**

Authors would like to thank Mr. P. R. Davange, Mr. R. S. Madhavi, Mr. D. V. Gaikwad, Dr. M. Kaur, Dr. N. Datta and Mrs. S. Kailasaganapthi for their help and support.

**References**

1. N. S. Ramgir, Y. Yang, M. Zacharias, Nanowire-Based Sensors, Small 6 (2010) 1705-1722.
2. N. S. Ramgir, P. K. Sharma, N. Datta, M. Kaur, A.K. Debnath, D.K. Aswal, S.K. Gupta, Room temperature H2S sensor based on Au modified ZnO nanowires, Sens. Actuators B 186 (2013) 718-726.
3. N. S. Ramgir, M. Ghosh, P. Veerender, N. Datta, M. Kaur, D.K. Aswal, S.K. Gupta, Growth and gas sensing characteristics of p- and n-type ZnO nanostructures, Sens. Actuators B 156 (2011) 875-880.
4. Niranjan S. Ramgir, V. Patnaik, A. Patel, A. K. Debnath, D. K. Aswal, S. K. Gupta, $SnO_2$ Thin film based electronic nose: A case study, Asian J. Physics, 24, 11 (2015) 1541-1548.

# Synthesis, Characterisation and Evaluation of Strontium Selective Crown Ether 4,4'(5') -[di t-butyldicyclohexano]-18-crown-6

**Snehasis Dutta, Sulekha Mukhopadhay and K.T. Shenoy**
Chemical Engineering Division
**S. Mohan**
Chemical Engineering Group

4,4'(5')-[di t-butyldicyclohexano]-18-crown-6 has been synthesised, as a highly selective ligand for $Sr^{90}$. The process involves the synthesis of 4,4'(5')-[di t-butyldibenzo]-18-crown-6 from which, 4,4'(5')-[di t-butyldicyclohexano]-18-crown-6 is synthesised by heterogeneous catalytic hydrogenation. This study portrays the role of the composition of the reaction medium on chemo-selectivity and yield of hydrogenation. The catalyst used in the hydrogenation i.e., 5% rhodium supported on γ-alumina, was synthesised in house and was characterised. Evaluation of the synthesised ligand was carried out through studies on extraction of Sr from simulated acidic high level waste. The synthesized ligand is found to be very effective for this role.

## Introduction

$Sr^{90}$ is produced as a fission product with its yield from $U^{235}$, $U^{233}$, and $Pu^{239}$ being 5.7%, 6.6%, and 2.0% respectively [1]. It is a emitter ($t_{1/2}$ 28.8 yrs, 0.546 MeV) and decays to $Y^{90}$, also a emitter ($t_{1/2}$ 64 hrs, 2.28MeV) which decays to stable $Zr^{90}$. Removal of $Sr^{90}$ and $Cs^{137}$ from High Level Waste (HLW) may eliminate the challenges of high decay heat in immobilisation of HLW. The commercial use of $Sr^{90}$ is also significant. $Y^{90}$, is used as a blood irradiator for treatment of bone cancer; $Sr^{90}$ has application as energy source at remote locations and in Radioisotope Thermoelectric Generator (RTG) in spacecraft.

High selectivity and affinity for strontium has led to the use of 4,4'(5')-[di t-butyldicyclohexano]-18-crown-6 (DTBDCH18C6) in recovery of Sr from radioactive waste solution [2]. With two tertiary butyl groups it has high oleophilicity. Also, its high radiation stability and low aqueous solubility makes it suitable to be used in commercial plant for Sr recovery. This ligand was first synthesised and used for the recovery of $Sr^{90}$, in 1990 [3, 4]. In this paper we elucidate the detailed synthesis of 4,4'(5')-[di t-butyldicyclohexano]-18-crown-6. The effect of the composition of the reaction media on the chemo-selectivity and yield of the hydrogenation reaction has been studied. The hydrogenation catalyst i.e., rhodium supported on γ-alumina was prepared using a novel route. This work also depicts the strontium extraction performance of the synthesized ligand from HLW. The effects of various organic diluents used in solvent extraction of strontium with the ligand, have been demonstrated.

The reaction is carried out in a glass reactor, with the drop-wise addition of a combination of KOH (1-2M) and tert-butyl catechol (TBC, 1M) in butanol, to a solution of bischloroethyl ether (BCE) dissolved in butanol. The reaction takes place in a nitrogen environment, under reflux condition at 116 $^0$C. The drop-wise addition of TBC is done in 2 steps, each addition step is carried out for 3-4 hrs and there is a time lag of 3 hrs between the steps. 24 hrs after the dropwise addition process, the reaction mixture is treated with KOH, and refluxed for additional 44 hrs. After which the excess KOH is neutralised by HCl addition, and butanol is recovered using a Rota-evaporator.

**Synthesis of 4,4'(5')-[di t-butyldibenzo]-18-crown-6 (DTBDB18C6) – '*the precursor*'**

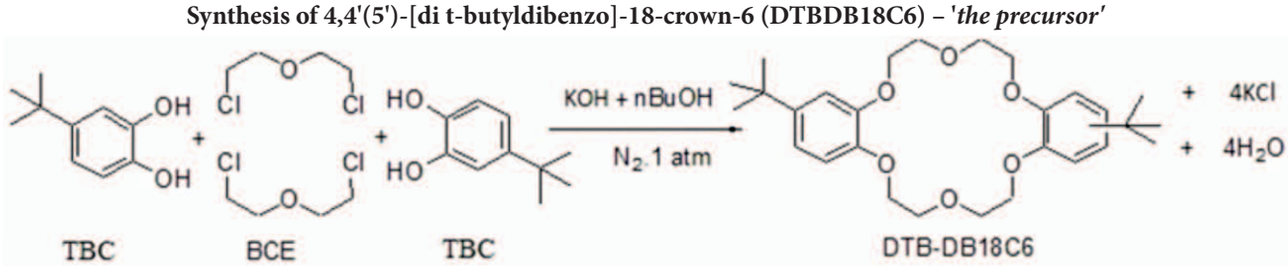


**Fig. 1: Reaction for the synthesis of 4,4'(5')-[di t-butyldibenzo]-18-crown-6**

**Purification of crude 4,4'(5')-[di t-butyldibenzo]-18-crown-6**

The product formed through the process discussed in the above section, is crude 4,4'(5')-[di t-butyldibenzo]-18-crown-6, containing about 16% (GC) of 4,4'(5')-[di t-butyldibenzo]-18-crown-6. It is purified using chromatographic technique. Alumina column, loaded with the crude, is eluted with a solvent of optimum polarity (10% Ethyl Acetate in Petroleum Ether). Analysis of the different eluted fractions has revealed that the nature of elution is diffusive, accordingly a procedure consisting three consecutive column purification units have been developed. This process resulted in a purity of 86.4% (GC), and the yield of 4,4'(5')-[di t-butyldibenzo]-18-crown-6 was 10-12%, which is obtained as a white solid. This compound is also reported to be highly efficient in recovery of $Tc^{99}$ from alkaline low level nuclear waste [5].

**Synthesis of supported rhodium catalyst for hydrogenation reaction**

Synthesis of 5% rhodium impregnated on γ-alumina support is carried out using microwave aided solvo-thermal reduction technique. Measured quantity of γ-alumina is impregnated with rhodium chloride (from aqueous solution $RhCl_3$); in a high temperature sonication bath. The impregnated alumina is dried under vacuum at 200$^0$C followed by calcination at 300 $^0$C, for 6 hours. Rh[III] is then reduced to Rh[0], in a microwave reactor, using ethylene glycol under reflux condition. The change of colour from red to black gives an indication about the reduction. Activation of the catalyst is carried out at 300$^0$C temperature under continuously purged hydrogen environment for 6 hours.

**Characterisation of the synthesised catalyst**

EDXRF (Xenematrix-EX 6600 SDD) analysis has shown that the surface has about 87.5 % rhodium along with traces of zinc and iron as impurities. $H_2$ chemisorptions (Thermo Electron Corp.) studies have showed that the specific hydrogen coverage (BET) is in the range 89.69 – 118.2 $m^2$/gm (Fig. 2.B). The nature of hysteresis in the isotherm (Fig.2.A) shows the presence of uniform meso-pores.

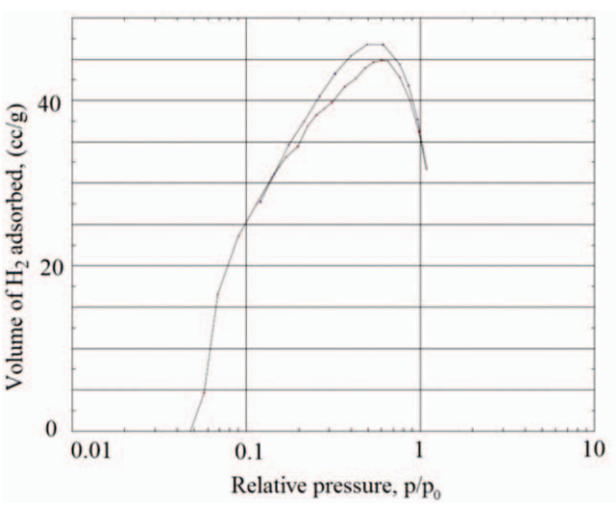


(A)

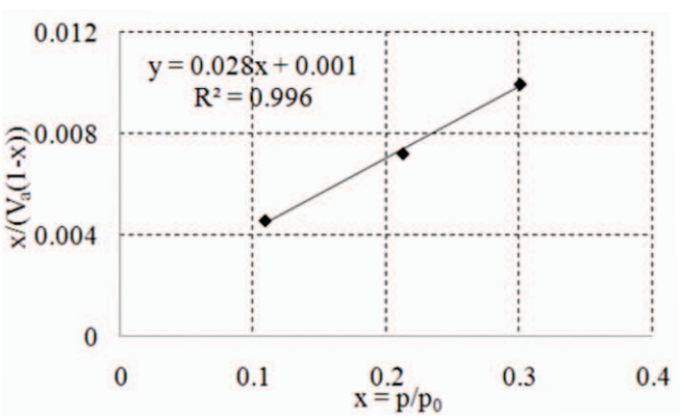


(B)

**Fig. 2: $H_2$ chemisorptions study of the synthesised catalyst; (A) Adsorption isotherm, (B) Plot of BET equation- 3 point method**

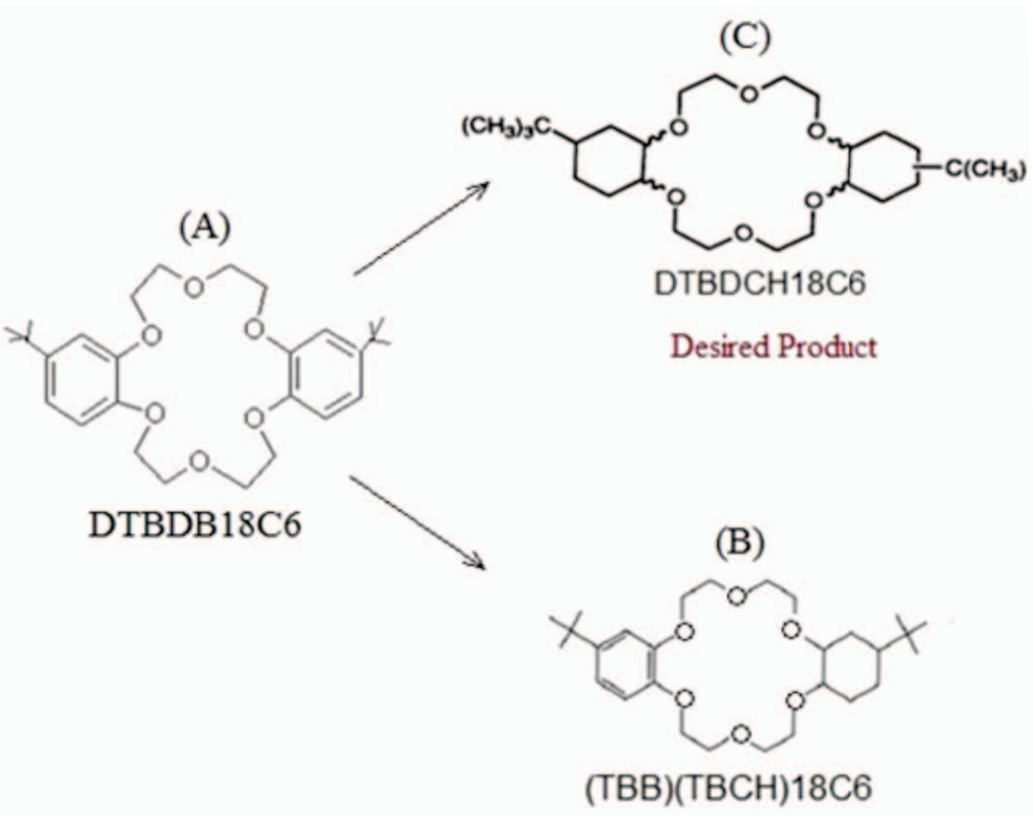


**Fig. 3: Catalytic hydrogenation of 4,4'(5')-[di t-butyldibenzo]-18-crown-6 (DTBDB18C6), to produce 4,4'(5')-[di t-butyldicyclohexano]-18-crown-6 (DTBDCH18C6) as the desired product; and (4-tertbutyl 2,3-Benzo) ((4')5'-tertbutyl 11,12-cyclohexano) 18-crown-6 ( TBB TBCH 18C6)**

**Removal of moisture from the reactant and the reaction media of hydrogenation reaction**

The reaction medium is n-butanol which is doubly distilled and is left to stand over molecular sieves (Sodium Alumino-silicate, 3Å, Finar). To enhance the polarity of the reaction media, valeric carboxylic acid is added to it [3]. It has comparatively long carbon chain (C5) which renders it to be hydrophobic in nature, thus it can be dried easily and stored without being attacked by moisture. Valeric acid is dried with anhydrous copper chloride, which is followed by vacuum distillation. DTBDB18C6 is dried by azeotropic distillation with benzene in a Dean-Stark collector [3].

**Catalytic hydrogenation of 4,4'(5')-[di t-butyldibenzo]-18-crown-6**

Catalytic hydrogenation of 4,4'(5')-[di t-butyldibenzo]-18-crown-6, has been carried out in autoclave of 50mL to 1 L capacity Stainless Steel (SS) 316 autoclaves. The ratio of the catalyst to the reactant is 1:5; the ratio of reactant to n-butanol was 1:10; the ratio of catalyst to valeric acid is 1:1. Temperature is maintained at 65 $^0$C, and pressure of hydrogen gas is maintained at 35-40 bar during the reaction. The reaction was allowed to take place for 40 hours. After which the reaction mixture is filtered to separate the catalyst. The solvent is removed through evaporation in vacuum. The product (now dark in colour) is dissolved in chloroform and passed through an alumina column, to remove washed out rhodium. After recovering chloroform from the eluted solution, the final product is obtained as a light coloured viscous liquid with 88% yield and 71.8% purity of desired product. The product is characterised by GCMS, FTIR and NMR analysis and found to be similar to the commercially available sample.

Figure 4.A shows the gas chromatogram peaks present in the hydrogenation product. It shows the presence of the hydrogenated product, DTBDCH18C6, the half hydrogenated product, (TBB)(TBCH)18C6 and traces of unreacted DTBDB18C6. Figure 4.B depicts the mass spectrum of DTBDCH18C6, with its mass peak (m/z) at 484. In figure 5.B, $H^1$-NMR of the synthesized ligand, shows the disappearance of the peaks with proton shift of 6.8-7.265, and the presence of peaks with proton shift of 1.2-1.274. Thus, $H^1$-NMR reveals that considerable amounts of phenyl group present in the reactant (Figure 5.A) have been hydrogenated. FTIR analysis of the synthesized ligand (Fig. 6) shows major peaks at 1098 $cm^{-1}$, 2780 $cm^{-1}$, 3310 $cm^{-1}$ for C-O, C=O and O-H respectively, similar to that reported in literature for DTBDCH18C6 [6].

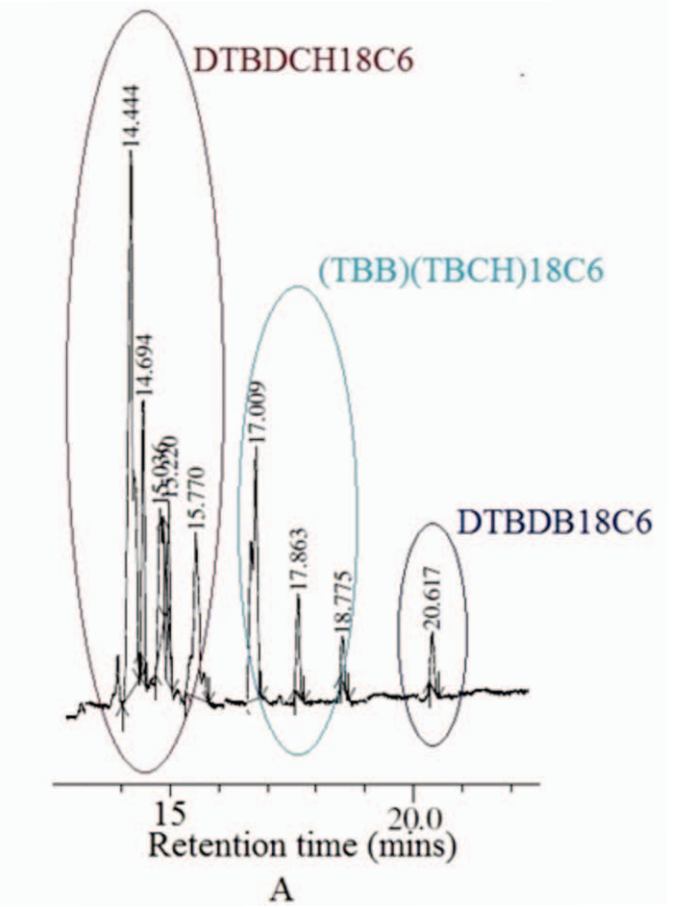


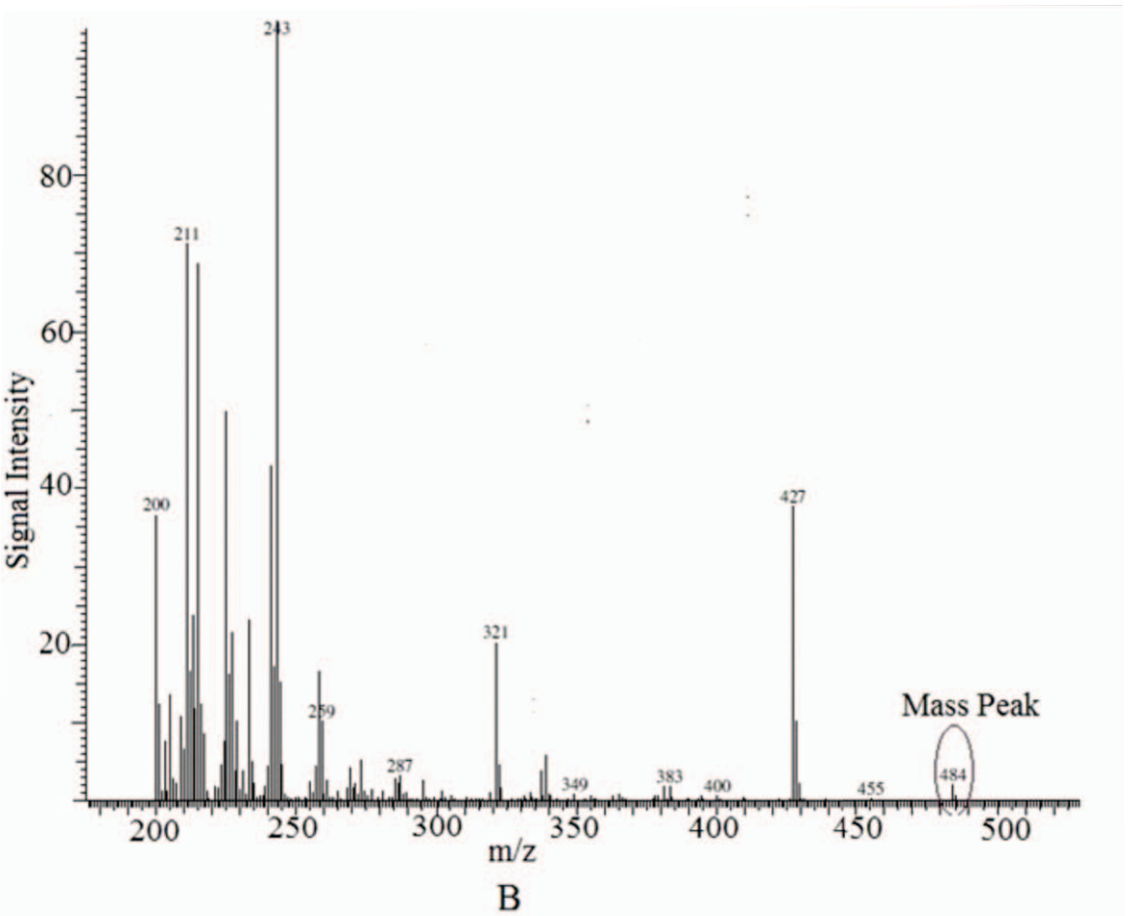


Fig. 4: GCMS analysis of the product (A) Gas chromatogram of hydrogenation product;
(B) Mass spectrum of 4,4'(5')-[di t-butyldicyclohexano]-18-crown-6

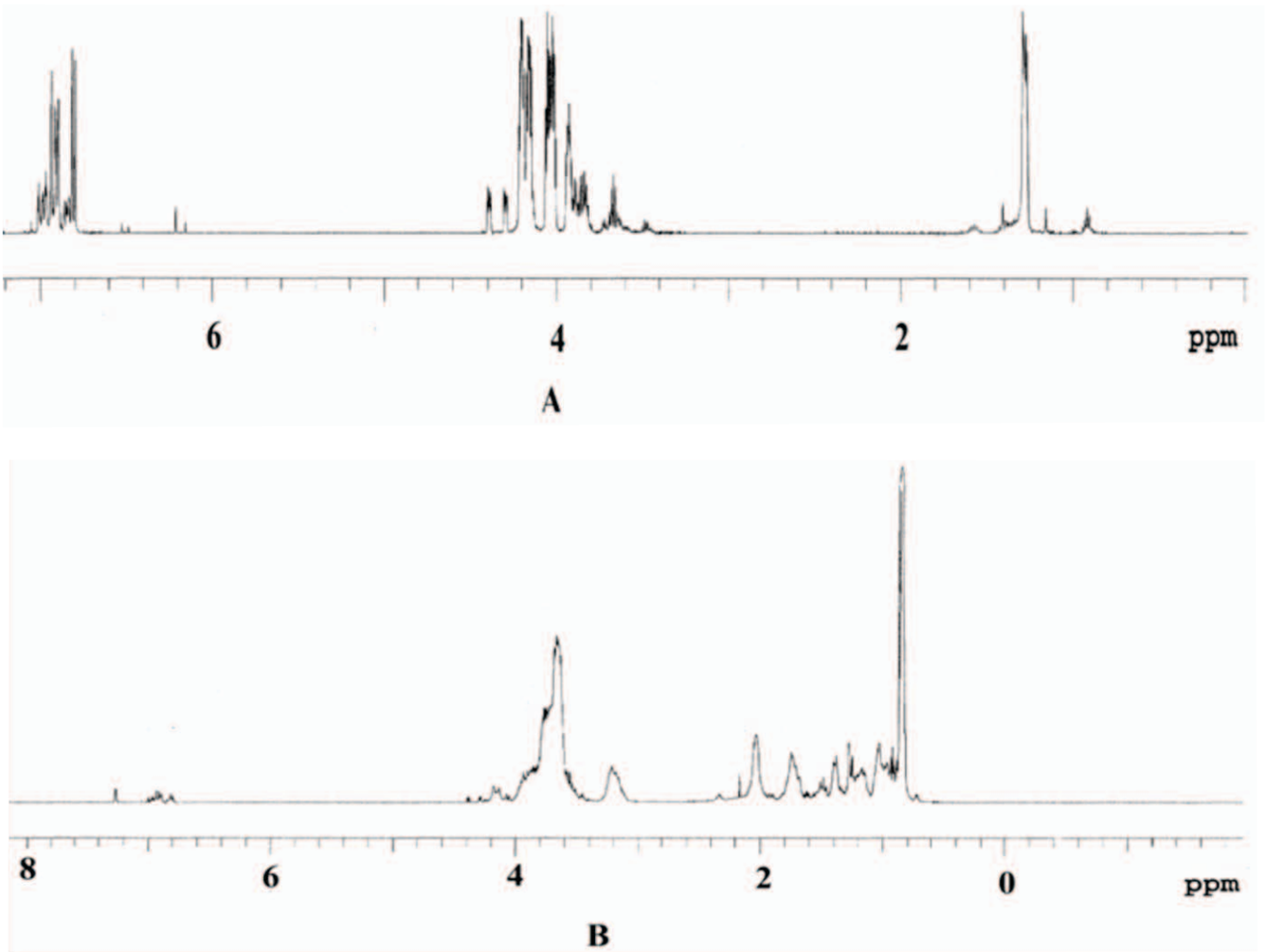


Fig. 5: $H^1$ NMR analysis, (A) Reactant, (B) Product

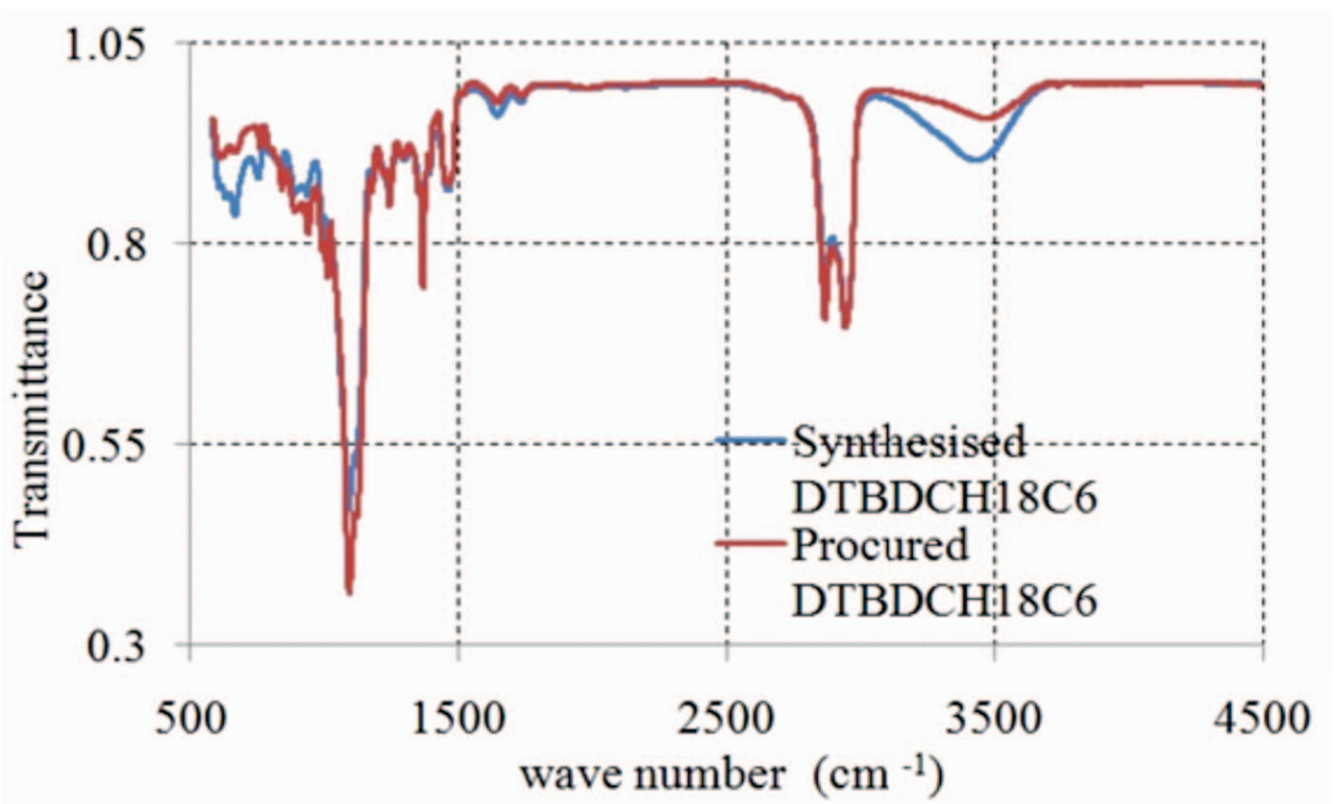


Fig. 6: FTIR analysis of synthesized ligand

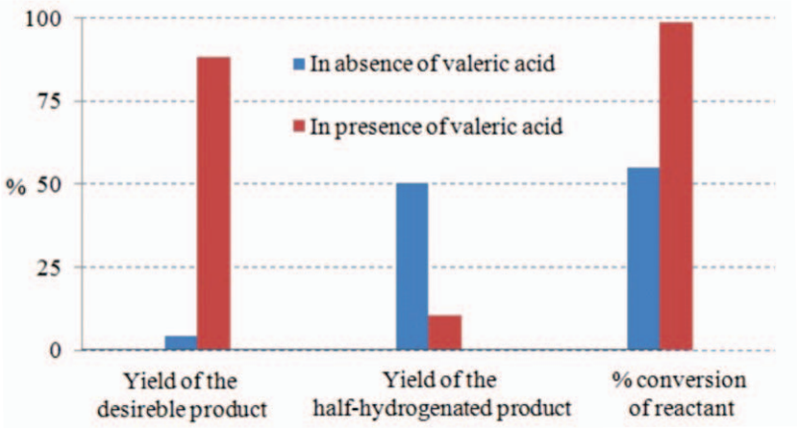


**Fig. 7: The effect of valeric acid in the hydrogenation reaction media**

### Effect of the composition of the reaction medium

The reaction is extremely sensitive towards the presence of moisture in reaction media, which prevents the reaction to take place. The presence of valeric acid in the reaction media has an enhancing effect on the yield and chemo-selectivity of the hydrogenation reaction which has been illustrated in Fig. 7. In absence of valeric acid, catalytic hydrogenation mostly yields the half hydrogenated crown ether, (TBB)(TBCH)18C6 i.e., B in Fig. 3; which results in a distribution coefficient of 1.7 for strontium in, 4N nitric acid solution, with 0.2M solution in octanol. On contrast, in presence of valeric acid the reaction proceeds to DTBDCH18C6 i.e., C in Fig. 3, which is the major product. The distribution coefficient of Strontium with this product was found to be about 13.6 under similar conditions. The most probable explanation to this observation may be that valeric acid enhances the polarity of the reaction media, which in turn increases the solubility of hydrogen in the reaction media.

### Evaluation of synthesised 4,4'(5')-[di t-butyldicyclohexano]-18-crown-6

The synthesised compound was tested for its ability to extract strontium from acidic solution. It is dissolved in organic diluents and contacted with 30-45 ppm Strontium in 4M nitric acid, for 10 mins. The distribution coefficient of strontium, for various diluents is depicted in Fig. 8. The product was found to be soluble in conventional solvents, like dodecane, isodecanol, octanol etc. The maximum distribution coefficient of 22.47 was obtained with 0.2M solution of the synthesized ligand in 1:1 mixture of dodecane and isodecanol with pure strontium nitrate feed solution. 85-90% stripping was obtained, with three contacts of Demineralised Water (DM).

Distribution coefficient for Sr, Am, Pu, Cs in simulated radioactive waste was found to be about 7.26, 0.01, 0.26, and 0.1 respectively. These experiments were carried out with 0.1M DTBDCH18C6 in octanol, in Waste Immobilisation Plant (WIP) Lab, Mumbai. Accordingly, the selectivity for strontium was found to be greater than 48.

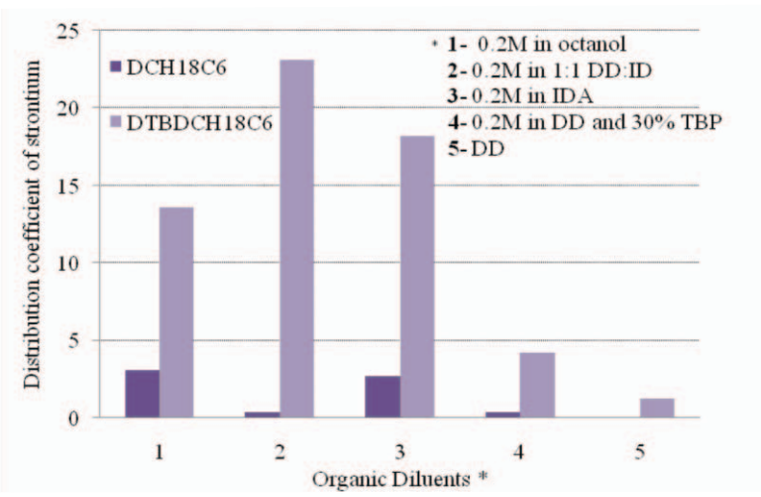


**Fig. 8: Comparison of the performance of the synthesised ligand with previously used ligand, DCH18C6 in different organic diluents**

## Conclusion

4,4'(5')-[di t-butyldicyclohexano]-18-crown-6 was synthesised in batches ranging from 3- 43 grams in 50 mL to 1L SS autoclave. NMR, GCMS and FTIR characterisation identifies the synthesised ligand as 4,4'(5')-[di t-butyldicyclohexano]-18-crown-6. The hydrogenation reaction is found to be sensitive to the polarity of the medium which is enhanced by presence of C5 carboxylic acid. The synthesised 4,4'(5')-[di t-butyldicyclohexano]-18-crown-6 is found to have high distribution coefficient and high selectivity (>45) for strontium w.r.t. impurities like americium, plutonium, cesium etc present in acidic high level nuclear waste. The precursor 4,4'(5')-[di t-butyldicyclohexano]-18-crown-6 was synthesised in 400 gm batch with about 86% purity and 10% yield.

## References


1. "Livechart - Table of Nuclides - Nuclear structure and decay data". IAEA, 2014.
2. Baisden, P., A., and Choppin, G., R., (2007),Nuclear Waste Management and the Nuclear Fuel Cycle, in Radiochemistry and Nuclear Chemistry, [Ed. Sándor Nagy], in Encyclopedia of Life Support Systems (EOLSS), Developed under the Auspices of the UNESCO, Eolss Publishers, Oxford,UK, [http://www.eolss.net].
3. Gula, M., Bartsch, R., A., Process for the preparation of cis-syn-cis 4,4'(5')-[di t-butyldicyclohexano]-18-crown-6, US005478953A,1994.
4. Horwitz, E., P., Dietz, M., L., Process for the recovery of strontium from acid solutions, US 5100585 A, 1990.
5. Bonnesen, P., V., Moyer, B., A., Parsley, D., J., Armstrong, V., S., Haverlock, T.,J., Counce, R., M., Sachleben, R.,A., Alkaline side extraction of technitium from tank waste using crown ether and other extractants, Chemical and Analytical Sciences Division, ORNL/TM-13241, 1996.
6. Shaikh,Y., Lai, E., P., C., Sadi, B., Li, C., magnetic nano-particles Impregnated with 18-Crown-6 Ether: hybrid material synthesis for binding and detection of radioactive strontium, Nanosci. Technol., 2(1):1-5, 2015.


## Acknowledgement

The authors profusely acknowledge the help and support from Waste Immobilisation Plant, Nuclear Recycle Group, Mumbai for evaluating the synthesised ligand with radioactive samples. The help and support from Bio-Organic Division, BARC for $H^1$-NMR, and High Pressure and Synchrotron Radiation Physics Division for FTIR analysis of the organic samples. The authors deeply thank Heavy Water Division, BARC, for helping with the $H_2$ chemisorptions studies of the catalyst. The authors are grateful to LSS, ChED for providing analytical support for inactive samples of Sr.

## Abbreviations

| | |
|---|---|
| DCH18C6 | Dicyclohexano-18-crown-6 |
| DD | Dodecane |
| ID | Isodecanol |
| TBP | Tri-n-butyl phosphate |

# महत्वा कांक्षी भारत को बिजली उपलब्ध करना

डॉ. आर. बी. ग्रोवर

**बिजली की आवश्यककता का अनुमान लगाना**

अक्सीर यह सवाल किया जाता है कि "भारत को कितनी बिजली की आवश्य कता है।" इसका जवाब देने के लिए हमें टॉप-डाउन अर्थमितीय मॉडल के अनुसार, हमें अर्थ व्यवस्थार में बढ़ोतरी की जांच, आर्थिक वृद्धि और ऊर्जा आवश्य कता के बीच के संबंध तथा प्रौद्योगिकी एवं नीति परिवर्तनों के प्रभाव को शामिल करते हुए विश्लेकषण करना पड़ेगा। वैकल्पिक बॉटम-अप मॉडल के अनुसार, हमें उपस्क्र की परिपूर्णता, कुशलता एवं उपयोग के आधार पर बिजली की मांग का पूर्वानुमान लगाना होगा। इस प्रकार, पूर्वानुमान के लिए कई धारणाओं का प्रयोग किया जाता है जिनका चयन विश्लेरषण से जुड़े समूह या व्यक्तित पर निर्भर रहता है। एक आशावादी व्यक्तिक ऊर्जा दक्षता में उच्चर जीडीपी विकास दर और महत्वकपूर्ण लाभों का चुनाव करेगा, जबकि एक रूढ़िवादी व्यक्तिक विपरीत काम करेगा। इस प्रकार, पूर्वानुमान के अध्यलयन के परिणाम इस प्रकार केवल संकेतक होते हैं, लेकिन वे प्रवृत्तियों को सामने लाते हैं और योजना के लिए उपयोगी होते हैं। लेखक ने अतीत में योजना के लिए भविष्यव परिदृश्यों पर काम किया है और इस तरह के परिदृश्योंख पर काम करना जारी रखा है ताकि संभावित विकास पैटर्न की जानकारी मिल सके।

बिजली की मांग के विकास का अनुमान लगाने के लिए, एक सरल विधि है आस पास के देशों में मांग का अवलोकन करते

हुए निष्किर्ष पर पहुंचना। वर्ष 2014 में अंतर्राष्ट्री य ऊर्जा एजेंसी द्वारा प्रकाशित आंकड़ों के अनुसार, औसत वैश्वि क प्रति व्यक्तिर वार्षिक बिजली की खपत 3052 kWh (kWh बोलचाल की भाषा में एक इकाई के रूप में जाना जाता है।) थी। भारत के लिए यह आंकड़ा लगभग 859 था जबकि ओईसीडी समूह के विकसित देशों के लिए यह 8016 था।

ओईसीडी समूह के अधिकांश देश समशीतोष्ण जलवायु क्षेत्र में हैं। इसलिए, आइए, हम भारत के समीप के दृश्यक की जांच करें। सिंगापुर के लिए यह आंकडा था 8849, मलेशिया 4656 और थाईलैंड के लिए 621 था।

अंतर्राष्ट्री य परमाणु ऊर्जा एजेन्सी (IAEA) द्वारा प्रकाशित रिपोर्ट के अनुसार शतक के मध्यए तक औसत वार्षिक वैश्विक प्रति व्यक्ति खपत 7500 यूनिट होगी और इसके समानुरूप मध्यट पूर्व एवं दक्षिण एशिया में 8400 यूनिट होगी। इन सब आंकड़ों की सहायता से हम भारत के लक्ष्य का निर्धारण कर सकते हैं।

**प्रति व्यक्ति उत्पादन हेतु लक्ष्यल निर्धारित करना**

उद्योग तथा घरेलू उपकरणों की ऊर्जा दक्षता की वृद्धि पर जोर देते हुए ऊर्जा संरक्षण से बिजली की खपत को कम किया जा सकता है, परंतु OECD देशों के नागरिक जिस जीवन स्त र का आनंद ले रहे हैं उस स्तएर का आनंद लेने के लिए लगभग 5000 यूनिट प्रति वर्ष से घटाना मुश्किल लगता है। यह मानते हुए कि सदी के मध्य तक भारत की जन संख्या 1.6 अरब तक होगी और प्रसारण तथा वितरण ह्रास को तकनीकी रूप से संभव निम्न तम 7% तक लाया जाए तो भारत को अपने नागरिकों को प्रति वर्ष प्रति व्यक्तिव को 5000 यूनिट उपलब्धध कराने के लिए लगभग 8600 बिलियन यूनिट (BU) उत्पातदन करने की योजना बनानी होगी।

वर्ष 2016-17 में उपयोगिताओं द्वारा उत्पादन 1242 BU रहा। गैर उपयोगिताओं से उत्पादन के आंकडे अभी तक उपलब्ध0 नहीं हैं, लेकिन अनुमान के लिए यह कहा जा सकता है कि उत्पागदन 2015-16 के समान अर्थात 168 BU होगा । इस प्रकार कुल उत्पामदन 1410 BU रहा । 1.3 बिलियन की आबादी मानते हुए, यह 1100 यूनिट प्रति व्यक्ति उत्पातदन दर्शाता है। 2006-07 से 2015-16 की अवधि के लिए भारत में बिजली उत्पारदन की संचयी औसत वृद्धि दर (सीएजीआर) 6% के करीब थी। 1410 बीयू के आधार से और 6% CAGR से शुरू करते हुए यह निष्कदर्ष निकाला जा सकता है कि सदी के मध्यब में प्रति वर्ष 8600 BU प्रति वर्ष का लक्ष्यय पार करना संभव है।

इस प्रकार, 2050 के लिए अनुमानित बिजली उत्पाकदन 2016-17 में कुल उत्पाओदन का छह गुना है और प्रति व्यक्ति उत्पानदन के मामले में यह लगभग 4.5 गुना है। भारत को एक लंबा रास्ता तय करना है।

प्रति वर्ष प्रति व्यक्तिप 5000 यूनिट की उपलब्ध ता का लक्ष्य कई कारणों से बहुत साधारण है। कई कारणों में से एक है कुल ऊर्जा खपत में बिजली की खपत की प्रतिशतता में लगातार वृद्धि, जो कि उपयोगकर्ताओं को इससे प्राप्तर होने वाली स्व च्छशता व सुविधा से संबंधित है। अनुमानों के अनुसार, प्रतिशतता वर्ष 2015 के दौरान मध्य पूर्व एवं दक्षिण एशिया में 34.8% थी और वर्ष 2050 तक इसके 52% तक बढ़ने की संभावना है। भारत सरकार सभी के लिए बिजली और आवास, त्विरत अवसंरचना विकास, मेक इन इंडिया, परिवहन का विद्युतीकरण आदि क्षेत्रों में पहल कर रही है। इन सभी के लिए विश्वंसनीय आधार पर अधिक बिजली की उपलब्धतता की आवश्यलकता होगी।

**महत्वातकांक्षी अपेक्षाएं**

जीवन प्रत्यावशा बनाम प्रति व्यक्तिल बिजली की खपत जैसे कथानकों के आधार पर प्रति व्यक्तिक बिजली की आवश्यपकताओं के बारे में अनुमान लगाए गए हैं। लेकिन, दो प्राचलों के मध्यथ के सह संबंध को कारक के रूप में नहीं माना जा सकता। मितव्येयी जीवन शैली अपनाते हुए कम बिजली की खपत करने जैसी राय को अधिक मान्यमता नहीं दी जा सकती क्योंकि विश्वीस्तसर पर बिजली की खपत लगातार बढ़ती जा रही है। क्या कोई भारत के युवाओं से मितव्यजयी जीवनशैली अपनाने की आशा कर सकता है ? महत्वा कांक्षी भारत की अपेक्षा है वातानुकूलित स्थाननों में काम करना और जीना, विद्युत उपकरणों के प्रयोग से घरेलू कार्यों में नीरसता एवं श्रम को कम करना, अपने मनोरंजन के लिए उत्कृऔष्ट थियेटर सिस्टकम का प्रयोग करना, दोस्तोंत एवं संबंधियों से जब चाहे बातें करना,

प्रदूषण रहित परिवहन में सुविधाजनक रूप से यात्रा करना आदि एक बार मूलभूत सुविधाएं उपलब्धा हो जाने पर एक सामान्यन भारतीय एक महत्वांकांक्षी भारतीय बन जाएगा।

विद्युत प्रकाश और इनडोर जलवायु नियंत्रण के कारण मानव जीवन अधिक उत्पायदक बन गया हैं। इलेक्ट्रिक बल्बय ने, दिन हो या रात, काम के स्था नों और घरों के अंदर प्रकाश व्यहवस्थाक पर मनुष्यों को नियंत्रण प्रदान किया। विश्वक के ठंडे क्षेत्रों के प्रदेशों में जलवायु नियंत्रण के लिए इनडोर हीटिंग से उत्पाहदकता में बढ़ोतरी हुई है और भारत सहित उष्णजकटिबंधीय देशों में वातानुकूलन से यह संभव हो रहा है। जैसे-जैसे ग्रीनहाउस गैस मौसम पैटर्न को प्रभावित करेगा, वैसे-वैसे इनडोर जलवायु नियंत्रण की आवश्यरकताएं बढ़ेंगी।

**सभी वैकल्पिक स्रोतों का उपयोग करें**

इस पृष्ठ्भूमि को देखते हुए हमें अपने लिए उपलब्धल सभी ऊर्जा स्रोतों को देखना होगा, बेशक निम्नो कार्बन ऊर्जा स्रोतों को प्राथमिकता दी जानी चाहिए जैसे कि बड़े पनबिजली, सौर ऊर्जा, पवन ऊर्जा एवं परमाणु इत्यादि। बृहत पनबिजली से पिछले वर्ष 122 BU का उत्पा दन किया गया था। भारत में बृहत पनबिजली की क्षमता 122 BU तुलना में काफ़ी अधिक है, लेकिन अतिरिक्त क्षमता के दोहन में समय लगेगा।

नीति आयोग की रिपोर्ट में कहा गया है कि सौर एवं पवन ऊर्जा क्षमता क्रमश: 750 गीगावट है और 302 गीगावाट से अधिक है । 20% की क्षमता को मानते हुए यह 1, 840 BU उत्प1न्नB कर सकता है। ये संख्यारएं केवल अनुमानित हैं परंतु इससे यह स्पष्ट होता है कि बड़े जलविद्युत, सौर एवं पवन ऊर्जा से कुल उत्पादन, अनुमानित 8600 BU लागत का अधिक से अधिक एक चौथाई ही हो सकता है।

भारत की शेष बिजली कहां से मिलेगी? नाभिकीय ऊर्जा द्वारा उत्प न्नह बिजली की भागीदारी को यथाशीघ्र बढ़ाना होगा और निम्ना कार्बन स्रोतों पर आधारित संस्थाापित क्षमता में वृद्धि होने तक, जीवाष्म ईंधनों को अपनी भूमिका जारी रखनी होगी। बिजली के संयोजन को निर्धारित करने में बिजली की लागत की भी भूमिका होगी और इस लागत की संरचना जटिल है।

**बिजली की लागत**

बिजली की लागत को तीन भागों में विभाजित किया जा सकता है:- संयंत्र स्तार लागत, ग्रिड स्तढर लागत एवं अन्यी लागत। संयंत्र स्तवर लागत में पूंजी, प्रचालन एवं अनुरक्षण तथा ईंधन भरण शामिल हैं। पूंजीगत लागत ऋण पर ब्याज एवं इक्विटी पर रिटर्न के रूप में उत्पादन के लागत में उभरता है। नाभिकीय विद्युत संयंत्रों के लिए, पूंजीगत लागत अधिक है परंतु ईंधन भरण लागत कम है। सौर एवं वायु की पूंजीगत लागत लगातार घटती जा रही है और ईंधन भरण की लागत शून्यर है।

**ग्रिड स्त र लागत**

विद्युत ग्रिड के माध्यतम से उपभोक्ताह तक पहुंचना है और एक ग्रिड बिछाने के लिए ठोस निवेश की जरूरत है। वितरक उत्पादक से बिजली खरीदता है और प्रसारण और वितरण शुल्के, तकनीकी नुकसान की वसूली शुल्कर, प्रचालन व्यिय जोड़कर अपने मुनाफे को निर्धारित करते हुए ग्राहक से वसूली जाने वाली टैरिफ तय करता है। चूंकि विविध तकनीकों पर आधारित कई जनरेटर ग्रिड से जुड़े हुए होते हैं अत: ग्रिड एवं ग्रिड प्रबंधन नीतियां जनरेटर के चलन को प्रभावित करती हैं। इस प्रभाव को सिस्ट म इफेक्टध कहा जाता है। वर्तमान में विद्युत बाजार द्वारा सिस्ट म इफेक्ट का कोई मूल्य निर्धारण नहीं किया जाता।

हाल के वर्षों में वायु और सौर पर आधारित एक बड़ी क्षमता ग्रिड से जुड़ी है। वायु और सौर ऊर्जा चर अक्षय ऊर्जा (VRE) स्रोत हैं। VRE स्रोत आंतरयिक है परंतु इनकी ईंधन भरण लागत शून्यर होने के कारण इन्हें। ग्रिड को ऊर्जा देने में प्राथमिकता दी जाती है। ग्रिड प्रबंधक को यह सुनिश्चिईत करना होगा कि जब सायंकाल के समय सूर्य का प्रकाश उपलब्धथ न होने पर पर्याप्तग प्रेषण योग्यश उत्पागदन क्षमता ग्रिड के साथ जुड़ी हो ताकि अत्यगधिक मांग (Peak load) को पूरा किया जा सके। कोयला एवं नाभिकीय जैसी बेस लोड तकनीकों तथा बृहत पन-ऊर्जा, जो मौसमी आधार पर उपलब्धक होती है, द्वारा प्रेषणीय ऊर्जा उपलब्ध कराई जाती है।

ग्रिड स्तपर लागतों के घटक है: ग्रिड कनेक्शंन, ग्रिड विस्ताणर एवं पुनर्बलन, लघु कालीन तुलन लागत तथा पर्याप्ता बैकअप सप्लारई बनाए रखने के लिए दीर्घकालीन तुलन लागत । VRE स्रोतों के लिए बैकअप, ग्रिड कनेक्श न एवं पुनर्बलन लागत बहुत अधिक होती है। इस पहलू के प्रति नीति बनाने के दौरान ध्यान देने की आवश्येकता है ताकि VRE स्रोतों के सकारात्मरक पहलुओं का पूरा लाभ उठाया जा सके।

दिसंबर, 2016 में केंद्रीय विद्युत प्राधिकरण ने राष्ट्रीय बिलजी योजना मसौदा (DNEP) जारी किया जिसमें सिस्टरम इफेक्ट0 एवं परिणामत: सिस्टधम लागत का कई जगह संदर्भ है। ऊर्जा भंडारण में निवेश किये बिना VRE स्रोतों पर जोर देना प्रेषणीय उत्पापदन केंद्रों के लिए प्रति दिन लोड़ प्रोफ़ाइल को एक 'Duck Curve' में बदल देता है। इसके कारण प्रेषणीय उत्पादकों के क्षमता गुणक कम हो जाते हैं। DNEP का कहना है कि केवल भंडारण युक्ते छत पर लगी हुई सौर संस्था पनाओं के प्रयोग से ही अत्या धिक मांग को कम किया जा सकता है। यह VRE स्रोतों के ग्रिड के साथ समाकलन द्वारा उत्पपन्नस तकनीकी एवं प्रचालन चुनौतियों को स्वी कारता है। यह संयुक्तय साइकिल संयंत्रों के उत्पासदन क्षमता का ह्रास, उच्चन अनुरक्षण लागत तथा साइकिलिंग एवं रैम्पिंग के कारण होने वाले उच्चा उत्स र्जन को भी सामने लाता है। इसमें VRE स्रोतों के ग्रिड समाकलन लागत के केवल गुणात्मनक विवरण दिए गए हैं।

OECD की नाभिकीय ऊर्जा एजेन्सी द्वारा सिस्टाम इफेक्टो की मात्रा ठहराई गई है । जर्मनी से प्राप्तो डाटा पर आधारित, OECD रिपोर्ट कहती है, 10% प्रवेश पर सौर द्वारा उत्पा दन की लागतह रु. 2.28 प्रति यूनिट के समान है। इसी प्रकार नाभिकीय हेतु रु. 0.02, कोयले के लिए 0.01 प्रति यूनिट एवं गैस के लिए इससे भी कम है। इसके अलावा VRE स्रोतों के लिए बढ़ते हुए प्रवेश के साथ यह और भी बढ़ती जाएगी। प्राकृतिक गैस अथवा पंप भंडारण सुविधाओं जैसी स्रोतों की उपस्थिति के अनुसार सिस्टपम लागत प्रत्येयक देश में भिन्नर भिन्नं होती है। VRE स्रोतों की सही लागत समानता तभी प्राप्त् की जा सकती है जब उत्पायदन लागत एवं सिस्टकम लागत का जोड़ प्रेषण स्रोतों से मेल खाता हो।

अगस्तं, 2017 में ऊर्जा विभाग (DOE), यूएसए द्वारा बिजली बाज़ार एवं विश्वकसनीयता पर एक स्टा फ़ रिपोर्ट जारी की गई थी

जो सचिव, डीओई के अनुरोध के उत्तार में था। सचिव, डीओई अपने दिनांक 23 अगस्तस, 2017 के कथन में आशा व्यचक्त करते हैं कि यह रिपोर्ट ग्रिड की विश्व सनीयता एवं लचीलता के बारे में महत्व0पूर्ण आधार बनेगी। डीओई रिपोर्ट में दिया गया है कि मूल्य निर्धारण तंत्र या नियमन ईंधन एवं प्रौद्योगिकी से स्वलतंत्र हो तथा सेवाओं की उपलब्धेता की विश्व सनीयता पर आधारित हो। रिपोर्ट कहती है कि समाज बिजली पूर्ति के कई ऐसे गुणों का आदर करता है, जिनका मूल्यांकन बिजली व्या।पार में आज नहीं हो रहा है। यह VRE स्रोतों को दी जाने वाली प्राथमिकता को ओर इशारा है। रिपोर्ट में दिया गया है कि सौर ऊर्जा के ग्रिड में प्रवेश परिवर्तित होने के परिणामस्वकरूप, दैनिक लोड प्रोफ़ाइल 'Duck Curve' में परिवर्तित हो जाता है और यह कहा गया है कि जडत्वर, जो ताप विद्युत संयंत्रों में मौजूद रोटेटिंग मास के कारण होता है, अस्थिरताओं को निवारता है। सौर संयंत्रों में जडत्व नहीं होता ।

**अन्य लागत**

अन्यर लागतों में बिजली उत्पा दन से स्वास्यCu संबंधित बाह्य लागत, नयी उत्पासदन क्षमता के कारण विद्यमान उत्पातदन क्षमता पर प्रभाव, दुर्घटना के प्रभावों को निवारने की लागत, आपूर्ति को सुरक्षा तथा समाज को उपयोगी ऊर्जा मिलना शामिल है। अगस्त्, 2017 में प्रकाशित आर्थिक सर्वेक्षण 2016-17 के दूसरे खंड में ग्रिड स्तोरलागत और कुछ अन्यम लागतों का अनुमान लगाने का प्रयास किया गया है। इस प्रकाशन में ग्रीन हाऊस गैस उत्सगर्जन की लागत को दर्शाने के लिए 'कार्बन की समाजिक लागत' (SCC) का नाम दिया गया है। यूएसए के अनुसंधानकर्ताओं द्वारा प्रकाशित एक लेख में, वर्ष 2015 के लिए भारत का SCC का अनुमान एक टन CO2 के लिए 2.91 यूएस डॉलर बताई गई है। सामाजिक लागतों में स्वाएस्यष संबंधी लागत, आंतरायिकता की लागत, भूमि की विकल्पक लागत, सरकारी प्रोत्सांहनों की लागत तथा फंसी संपत्ति से उत्पंन्न लागतों को जोड़ा गया है। अत:, न केवल सिस्टपम लागत शामिल की गई है बल्कि अन्यं लागतों के महत्वमपूर्ण भाग भी इसमें शामिल हैं। प्रकाशन में अनुमान दिया है कि अक्ष ऊर्जा स्रोतों की कुल सामाजिक लागत रु.11/- प्रति यूनिट है जो कोयले से करीब तीन गुनी है।

**'प्रौद्योगिकी बनाम प्रौद्योगिकी' चर्चा का अन्त करें**

आस्ट्रेनलिया एवं केलीफ़ोर्निया, यूएसए VRE स्रोतों की आन्तकरायित्ताप की समस्या को हल करने के लिए बैट्री प्रणालियों को अपना रहे हैं। यूरोप में जनवरी, 2017 में बिजली की कीमत आसमान पर थीं क्योंरकि तब वहां सौर एवं पवन दोनों उपलब्धप नहीं थे। हाल ही के सप्तांहों में भारत में भी हाजिर भाव (spot price) में उछाल हो रहा था। इससे यह इंगित होता है कि तकनीकी विकास एवं नीति परिवर्तन में और अधिक कार्य करना होगा। VRE स्रोतों के अधिक उपयोग के लिए ऐसी योजना बनानी होगी जिससे अर्थव्यकवस्था। पर दुष्प्र भाव न पड़े। भारत को प्रौद्योगिकी बनाम प्रौद्योगिकी पर बहस नहीं चाहिए लेकिन ऐसी नीति की आवश्यथकता है जिसमें सभी निम्नक कार्बन प्रौद्योगिकियों अर्थात नाभिकीय एवं अक्षयों को कोयले के साथ इस प्रकार समाहित की जाए कि बिजली आपूर्ति की विश्वअसनीयता, सुरक्षा एवं वहन योग्य ता बनी रहे। सुनिश्चित बिजली आपूर्ति के लिए ईंधन एवं तकनीकों में विभिन्नरता जरूरी है।

**नाभिकीय ऊर्जा की भूमिका**

नाभिकीय ऊर्जा को देखें तो हाल ही के विकास ध्यान देने योग्या हैं। दिनांक 17 मई 2017 को मंत्रीमंडल ने प्रत्ये क 700 मेगावॉट के स्वधदेशी दाबित भारी पानी रिएक्टंर (PWHR) की दस यूनिटों के निर्माण को अनुमोदित किया है। इसके बाद कुडनकुलम में प्रत्येदक 1000 मेगावॉट के दो और रिएक्टRरों के स्थादपन हेतु 1 जून को रशिया के साथ सामान्यब समझौते पर हस्ताभक्षर किए गए। संयुक्तऔ घोषणा में वर्ष 2014 के दौरान हस्तादक्षरित विजन दस्तावेज में दोनों पक्षों की वचनबद्धता को दोहराया गया। जिसमें नए स्थएल पर प्रत्ये क 1200 मेगावॉट के छ: रिएक्टमरों का निर्माण शामिल है।

कुल 6780 मेगावॉट की संस्थापित क्षमता युक्त रिएक्टएर प्रचालनरत हैं। एक 500 मेगावॉट क्षमता वाला प्रोटोटाइप तीव्र प्रजनक रिएक्ट र (PFBR) कमीशनन के तहत है। प्रत्येरक 700 मेगावॉट क्षमतायुक्त चार PHWRs निर्माणाधीन हैं। वर्ष 2014 में 700 मेगावॉट वाले दो PHWRs की नीव रखी गई, और न्यूाक्लियर पॉवर कार्पोरेशन ऑफ इंडिया ने निर्माण की ओर पहला कदम रखा। कुडनकुलुम में 1000 मेगावॉट के चार रिएक्टटरों के निर्माण हेतु करार पर हस्तारक्षर किए गए और चार में से दो का निर्माण सरकारी तौर पर 29 जून, 2017 को पूरा हो गया और अधिक नाभिकीय विद्युत संयंत्रों के निर्माण हेतु यूएस एवं फ्रांस के साथ बातचीत जारी है।

**कार्यान्वयन**

लेखक को 11वीं पंचवर्षीय योजना प्रारंभ करने से पहले सरकारी बैठकों के दौरान क्षमता में वृद्धि का संवर्धन करने से संबंधित वार्तालाप याद है। कुछ विशेषज्ञों को भारत की लगभग 3000 मेगावाट प्रति वर्ष से अधिक क्षमता वृद्धि में सफलता के प्रति संदेह था। फिर भी, एक बार निर्णय लेने पर उद्योग द्वारा लक्ष्यरपूर्ति की गई और 11वीं योजना (2007-12) के दौरान कुल 50 गीगावॉट क्षमता जोड़ी गई। 12 वीं योजना (2012-2017) के दौरान इसे कुल 130 गीगावॉट कर दिया गया। इस क्षमता का प्रमुख भाग कोयला क्षेत्र में था। निम्न् कार्बन वृद्धि के प्रति वचनबद्धता को पूरा करने के लिए नाभिकीय संस्थापन क्षमता में वृद्धि की आवश्य कता है। कोयला क्षेत्र में प्राप्तन वृद्धि दर को देखते हुए, वर्ष 2032 तक 63 गीगावॉट नाभिकीय ऊर्जा में वृद्धि संभव है। इसके लिए परमाणु ऊर्जा विभाग, न्यूक्लियर पॉवर कॉर्पोरेशन ऑफ इंडिया (NPCIL) तथा भाविनी द्वारा एक स्प ष्टन योजना तैयार करनी होगी। इसमें उपस्कहर विनिर्माताओं को भी शामिल किया जाए। इस लक्ष्य को प्राप्तभ करने के लिए हाल ही के अनुमोदनों के साथ-साथ सरकार द्वारा इस प्रकार के और अधिक अनुमोदन दिए जाने चाहिए।

लेखक परमाणु ऊर्जा विभाग की होमी भाभा चेअर पर शोभायमान हैं और परमाणु ऊर्जा आयोग के सदस्यि हैं। इस लेख में दिनांक 15.07.2017 के 'इकोनोमिक टाइम्सए' तथा दिनांक 31.08.2017 एवं 03.10.2017 के 'दि हिंदु' में लेखक द्वारा प्रकाशित लेखों का पाठ्य शामिल है। हिंदी में अनुवाद करने के लिए लेखक हिंदी अनुभाग, भापअ केंद्र के आभारी हैं।

# National Technology Day 2017

BARC celebrates the National Technology Day (NTD) on May 11 to mark India's advancements in technology. Dr. S. Christopher, Chairman, Defence Research and Development Organisation (DRDO) and Secretary, Department of Defence Research & Development was the chief guest for the event. In the inaugural session, Shri K. N. Vyas, Director, BARC welcomed the chief guest and Dr. Sekhar Basu, Chairman, Atomic Energy Commission delivered the presidential address. Shri B. S. Jagadeesh, Associate Director, Electronics & Instrumentation Group (E&IG) and Head, Computer Division explained the significance of the National Technology Day to the audience. In his keynote address titled "Innovation – AEWACS programme: A Case Study" Dr. Christopher highlighted various innovations by the design team of the Airborne Early Warning and Control System in DRDO. Shri R. S. Mundada, formerly Associate Director E&IG and Convenor NTD - 2017 proposed the vote of thanks.

BARC organises a technological exhibition based on a certain theme to mark the National Technology Day. This year's theme is "Electronics and Computer Technology – Empowering the Nation". The chief guest inaugurated the exhibition in the Central Complex auditorium, which showcased exhibits and posters on various technologies and systems developed in BARC. The exhibition was visited by about 1000 students from different schools across Mumbai during May 11-14, 2017.

In the later part of the day, a technical session comprising of talks by the recipients of the Homi Bhabha Science and Technology Awards, 2015 was organised in the Supercomputing Facility auditorium. Dr. R. Mittal, Solid State Physics Division, BARC, Dr. A. K. Chaturvedi, Atomic Minerals Directorate for Exploration and Research, Dr. P. K. Mukherjee, Nuclear Agriculture and Bio-Technology Division, BARC, Dr. John Philip, Indira Gandhi Centre for Atomic Research and Shri S. B. Patil, Technology Development Division, BARC made their award winning presentations.

Further, BARC also arranged an exhibition in the DAE convention centre, Anushakti Nagar during May 13-14 for the benefit of the general public. Shri S. A. Bharadwaj, Chairman, Atomic Energy Regulatory Board inaugurated the exhibition. Infotainment shows and skits were staged to make it more interesting for the visitors here.


**Dr. S. Christopher, Chairman DRDO and Secretary, Dept. of Defence R&D, delivering the keynote address**

Inauguration of the exhibition on May 11

The Chief Guest at the exhibition on May 11

Inauguration of the exhibition on May 13

The Chief Guest at the exhibition on May 13

Visitors at the exhibition on May 13-14

Visitors at the exhibition on May 13-14

**Central Complex at BARC**

Edited & Published by:
Scientific Information Resource Division
Bhabha Atomic Research Centre, Trombay, Mumbai 400 085, India
BARC Newsletter is also available at URL:http://www.barc.gov.in